

13585

NATIONAL LIBRARY
OTTAWA



BIBLIOTHÈQUE NATIONALE
OTTAWA

NAME OF AUTHOR..... *MILAN SROKA*

TITLE OF THESIS..... *Design of an Atmospheric*
Testing Tunnel

UNIVERSITY..... *U. of A*

DEGREE FOR WHICH THESIS WAS PRESENTED..... *M. Sc.*

YEAR THIS DEGREE GRANTED..... *1972*

Permission is hereby granted to THE NATIONAL LIBRARY
OF CANADA to microfilm this thesis and to lend or sell copies
of the film.

The author reserves other publication rights, and
neither the thesis nor extensive extracts from it may be
printed or otherwise reproduced without the author's
written permission.

(Signed)..... *M. Sroka*

PERMANENT ADDRESS:
413 Mich. St.
Edmonton
.....

DATED..... *Oct 4*19 *72*

THE UNIVERSITY OF ALBERTA

DESIGN OF AN ATMOSPHERIC
ICING TUNNEL

by



MILAN SROKA

A THESIS

SUBMITTED TO THE FACULTY OF GRADUATE STUDIES AND RESEARCH
IN PARTIAL FULFILMENT OF THE REQUIREMENTS FOR THE DEGREE
OF MASTER OF SCIENCE

DEPARTMENT OF MECHANICAL ENGINEERING

EDMONTON, ALBERTA

FALL, 1972

THE UNIVERSITY OF ALBERTA
FACULTY OF GRADUATE STUDIES AND RESEARCH

The undersigned certify that they have read, and recommend to the Faculty of Graduate Studies and Research, for acceptance, a thesis entitled " Design of an Atmospheric Icing Tunnel," submitted by Milan Sroka in partial fulfilment of the requirements for the degree of Master of Science.

..... *C. S. Lock*
Supervisor

David Marsden

Edward Lozanski

Date *September 26, 1972*

ABSTRACT

An analysis of conditions leading to atmospheric icing, design and calibration of an experimental icing facility (FROST^{*} Tunnel), and preliminary experiments on atmospheric icing are presented. The principal variables that characterize icing, the thermodynamic state of icing environment, and the mechanism of the accretion process are discussed. The experimental part is to check capabilities of the FROST Tunnel as an icing study facility rather than reveal the physics of icing or to obtain experimental design data.

* FROST is an acronym for Fundamental Research On Solidification and Thawing.

ACKNOWLEDGEMENTS

The author wishes to thank the following for their contributions; Professor G. S. H. Lock for supervising this thesis, The National Research Council for the funds made available under Grant No. A-1672, Members of the Mechanical Engineering Shop (particularly Mr. T. Simpson) who aided in construction of the FROST Tunnel, Members of the U. of A. Technical Services Shop (particularly Mr. Günter Zillt) who aided in design and manufacturing of aluminium sections of the tunnel.

TABLE OF CONTENTS

CHAPTER		PAGE
I	INTRODUCTION	1
II	AN ANALYSIS OF CONDITIONS LEADING TO ATMOSPHERIC ICING	5
	2.1 Freezing of a Supercooled Drop	5
	2.2 The Dynamics of a Drop in Flight	7
	2.3 Accretion Process	9
	2.4 Conclusions	15
III	DESIGN OF THE FROST TUNNEL	16
	3.1 Contraction and Working Sections	20
	3.2 The Settling Chamber	23
	3.3 The Diffusers	27
	3.4 The Corners	31
	3.5 The Fan and Refrigeration	31
	3.6 FROST Tunnel Modifications	32
	3.7 The Spraying System	32
IV	INSTRUMENTATION, CALIBRATION, AND PRELIMINARY EXPERIMENT	37
	4.1 Velocity Measurement	37
	4.2 Temperature Measurement	38
	4.3 Turbulence Measurement	39

CHAPTER	PAGE
4.4 Droplet Size Distribution	
Measurement	39
4.5 Liquid-Water Content Measurement . .	42
4.6 The Experiment	43
4.7 Test Results and Discussion	44
V CONCLUSIONS AND RECOMMENDATIONS	51
5.1 Conclusions	51
5.2 Recommendations	52
REFERENCES	55
APPENDIX A: POWER LOSS CALCULATION	59
APPENDIX B: HEAT LOSS CALCULATION	68

LIST OF TABLES

TABLE		PAGE
3.1	LO- & SLO-SPEED Design: Contraction Shape Data	24
3.2	HI-SPEED Design: Contraction Shape Data . . .	25
4.1	Test Results	45

LIST OF FIGURES

FIGURE		PAGE
3.1	FROST Tunnel Layout	18
3.2	FROST Tunnel Layout: Basic Design (LO-SPEED)	19
3.3	Contraction Cone	22
3.4	Settling Chamber	26
3.5	FROST Tunnel Layout: SLO- & HI-SPEED Modifications	33
3.6	Spraying System	35
4.1	Droplet Sampler	40
4.2	Run No. 1: Ice Deposit after 30 Mins.	46
4.3	Run No. 2: Ice Deposit after 30 Mins.	46
4.4	Run No. 1: Microphotograph of a Spray Sample	47
4.5	Run No. 2: Microphotograph of a Spray Sample	48
5.1	Alternative Nozzle-Water Temperature Control Arrangement	53

CHAPTER I

INTRODUCTION

The presence of water droplets and moisture in a cold environment generally leads to icing i.e. the formation of ice or snow on exposed surfaces. The variety of surface shapes and sizes together with the variety of environmental icing conditions can be combined, basically, into three groups of practical significance and applicability associated with problems of:

- (1) Aircraft icing
- (2) Ship-board icing
- (3) Land-based structure icing

Man has experienced icing and its dangers for centuries, especially in his early exploration of northern seas. Icing on ships, which is usually due to freezing of the sea spray that is blown over the vessel, may result in a heavy ice deposit on most of the above-water parts of a ship. This ice accretion increases the topside weight of the ship thus raising the center of gravity and reducing the ship stability. In spite of this evidence, it was the danger of aircraft icing that brought researchers to systematic study of the atmospheric icing problems. Unfortunately, the results thus obtained could not have been applied to solve ship icing problems. This led to the

situation that in the 1960's while aircraft were safely flying under all possible meteorological conditions man was alarmed by the loss of trawlers in northern waters (e.g. loss of the steam trawlers Lorella and Roderigo off the north coast of Iceland in January 1955). Naturally since then ship-board icing problem has received much more attention.

Ice and frost coatings on land-based objects such as bridges, towers, buildings often threaten their structural integrity which again presents danger and hazard for man.

The principal variables involved in atmospheric icing are: wind speed, liquid-water content, droplet size, and temperature of the environment. These differ significantly in cases of aircraft, shipboard, and land-based structure icing. High altitude clouds have relatively low liquid-water content, small drop size, and low temperature. Moreover, these variables do not change drastically within such a cloud so that experimental simulation is easier to handle. Data on the range of meteorological variables pertinent to aircraft icing have been widely investigated. The data obtained indicate that a statistical relation exists between liquid-water content, mean droplet diameter, temperature, and pressure altitude [1]. Icing conditions at sea, characterized by relatively high liquid-water content, large droplet size, and high temperatures, are very complex.

They exist as a result or combination of following:

- (1) Wind generated sea spray
- (2) Freezing rain or drizzle (or wet snow)
- (3) Supercooled sea fogs

While cases (2) and (3) are more common in typical arctic waters, the case (1) often called "spindrift" is the most serious cause of icing on ships in northern waters. The "spindrift characteristics" are very unstable and locally may vary rapidly in time depending on the wind-speed, the heading of the vessel relative to the wind, the speed of vessel, etc. A detailed parametrical analysis [2] revealed that the number of variables pertinent to shipboard icing is much larger than the number of non-dimensional parameters characterizing the physical situation. Therefore experimentation on shipboard icing is an enormous task itself since any particular experiment can handle few parameters of limited range only. Although detailed and consistent experimental investigation has not yet been performed, there have been attempts to simply map dangerous regions where heavy icing can occur [3]. However, the data collected so far are insufficient to draw any practical conclusions since there is no definite knowledge a priori under what conditions dangerous icing can exist.

Freezing rain, drizzle, and wet snow or their combination are essentially responsible for heavy ice (snow) deposits on land-based objects and structures. Regarding

this same data on frequency of freezing precipitations have been collected [4]. This data can be used for rough estimates of dangerous situations on various locations (e.g. for Canada see reference [5]) but again there have been no attempts at systematic study or experimental simulation of icing situations under these conditions.

CHAPTER II

AN ANALYSIS OF CONDITIONS LEADING TO ATMOSPHERIC ICING

2.1 Freezing of a Supercooled Drop

The atmosphere can be considered, depending on pressure, temperature, and humidity, as an air-water vapour-water-ice mixture.

A water drop can exist in a "cold" environment (temperatures below freezing point of water) provided it is "supercooled". Strictly, the expression "supercooled drop" refers to a drop in the state of metastable equilibrium. This, however, is not common in literature and supercooling refers generally to the freezing point depression, regardless of the mechanism leading to it. Droplets of pure water, only a few microns in diameter can be supercooled down to -40°C in the laboratory [6]. At temperatures below -40°C droplets freeze spontaneously, but at higher temperatures they can freeze provided foreign particles - ice-nuclei are presented. Spontaneous freezing of pure water droplets or homogeneous nucleation is caused by small groups of water molecules becoming locked into ice-like configurations thus forming a nucleus for the ice phase. The probability of such molecular aggregates increases as the temperature is lowered.

Heterogeneous nucleation, i.e. freezing of a water drop being infected by foreign nuclei, has been widely investigated. Perhaps the most important result, which had not long been recognized, is that the freezing of a supercooled drop is a random process and a given drop has only a statistical probability of freezing at a particular temperature. For the median freezing temperature (temperature below which half the drops freeze) a linear relationship between the logarithm of the drop diameter (d) and the median freezing temperature (T) in Kelvin's scale has been discovered [7]. Thus:

$$\ln d = A - BT$$

where A and B are constants for particular sample of water used. The effect of rate of cooling on freezing temperature has also been investigated. Bigg [7] found that with the rate of cooling 0.05°C/min the freezing temperature of a 1 mm drop was about 2°C higher than the corresponding value for the rate of cooling 0.5°C/min.

The freezing temperature of a water drop is also influenced by the presence of salts in solution. It has been found [8], [9] that increasing concentration of various salts decreases freezing temperature in proportion depending upon the particular salt.

2.2 The Dynamics of a Drop in Flight

Consider a laminar flow of an air-water droplet suspension past a certain body. Suppose the body is a circular cylinder and the droplets are of uniform size, uniformly distributed, and big enough so that their inertia forces can not be disregarded. Particles of air would follow curved streamlines approaching the cylinder; the water droplets would move in straighter paths because of the inertia forces, which will be balanced by imposed (drag) forces of resulting relative motion between the air and the water droplets. Thus, some of the water droplets would reach the cylinder, others would by-pass it depending on their relative position to the centerline of the motion. The effectiveness of impaction, commonly called the collection efficiency, may be then expressed as the ratio of the number of droplets that actually reached the body to the number that would have reached it had they continued in straight lines instead of following their respective trajectories. If Stokes law holds (small particles) the trajectories of water droplets can be calculated from equation of motion for a drop:

$$m \frac{d^2 \vec{r}}{dt^2} = 6\pi\mu d \left(\vec{v} - \frac{d\vec{r}}{dt} \right) \quad (1)$$

where m is mass of the drop, \vec{r} is the position vector of the drop, \vec{v} is local air velocity, d is the drop diameter, μ is dynamic viscosity of the air. The above equation in

dimensionless form becomes:

$$Sk \frac{d^2 \vec{r}'}{dt'^2} + \frac{d\vec{r}'}{dt'} = \vec{v}'(\vec{r}') \quad (2)$$

where $Sk = \frac{2Re \rho d^2}{9\rho_a R^2}$

is Stokes number, Re is Reynolds number, ρ is density of water, ρ_a is density of air, R is cylinder radius,

$$\vec{r}' = \frac{\vec{r}}{R}, \text{ i.e. normalized radius-vector,}$$

$$\vec{v}' = \frac{\vec{v}}{V_0}, \text{ } V_0 \text{ being velocity of suspension far from}$$

the body,

$$t' = \frac{V_0}{R} t, \text{ i.e. normalized time.}$$

The system of equations (2) was numerically integrated by Langmuir and Blodgett [10] for the case of potential flow past cylinders and spheres. Levin [11] obtained an analytic solution for potential flows near stagnation point. Also case when $Re \ll 1$ has been attempted analytically. The case of droplets of larger dimensions has been investigated by Fuks [12]. All the above solutions are of limited validity since authors completely disregarded both the existence of a boundary layer at the body's surface and the transportation of droplets by turbulent fluid beyond the separation point.

2.3 Accretion Process

The previous discussion of nature of the freezing process of an individual water drop, its trajectory approaching an obstacle could, at best, lead to a definition of "initial conditions" - namely collection efficiency, thermodynamic state of the water droplets - upon which the accretion process begins.

When the supercooled droplets impinge on the surface they begin to spread, are nucleated, and begin to freeze. During the freezing process the latent heat of fusion has to be removed and, essentially, the rate of freezing and temperature attained by the deposit is determined by a balance between the rate at which the heat is liberated by the freezing droplets and the rate at which the heat can be transferred to the environment by forced convection and evaporation. Since the mean surface temperature of the deposit can not exceed 0°C there is for given conditions - air and drop temperature, air speed, and object size - a critical liquid-water concentration for which all the accreted droplets may be just frozen [13]. If the actual liquid-water concentration is lower than the critical value, all of the droplets freeze and the mean surface temperature of the deposit is below 0°C . If actual liquid-water concentration is above the critical value, the excess of water which can not be frozen is partially shed off into the stream and partially incorporated into the ice structure.

Thus, two principal ice growth regimes have been recognized: Dry growth regime (liquid-water concentration is less than the critical), and wet growth regime (liquid-water concentration is above the critical). As a result the following classification of ice deposits has been made [14], [15].

Rime (dry growth regime) is a milky granular deposit of ice formed by rapid freezing of supercooled water droplets as they impinge on objects and freeze mainly in an individual manner. It is lighter - the density could be as low as 0.1 g/cm^3 - softer, and less transparent than glaze, discussed below. Factors which favour rime formation are small drop size, slow accretion, high degree of supercooling and rapid removal of latent heat of fusion. Rime can be subdivided into two groups; soft and hard rimes, the latter generally referring to a rime deposited by denser supercooled clouds.

Glaze (wet growth regime) is a relatively transparent ice deposit formed by freezing of a film of supercooled water. Glaze is denser, harder, and more transparent than rime. Factors that favour glaze formation are large drop size, rapid accretion, less supercooling, and slow removal of latent heat of fusion. Glaze is often described as compact and spongy. Compact glaze - density close to 0.9 g/cm^3 - is formed when the supercooled water droplets have time to spread over the surface and form continuous film before freezing and heat transfer between the deposit and the

environment is such that the surface is in a "just-wet" condition, i.e. at 0°C , and all accreted water freezes. Spongy glaze - density $0.9 - 1.0 \text{ g/cm}^3$ - is formed when heat transfer between the environment and the deposit is not sufficiently rapid to allow all of the deposited water to freeze, i.e. only a fraction of it freezes immediately to produce a skeletal framework of ice that may retain three to four times its own mass of unfrozen water.

Consider a circular cylinder of diameter R moving with velocity V in a supercooled cloud of uniform droplet size and distribution: let w be the liquid water concentration of the cloud and E the collection efficiency of the deposition process. The rate at which heat is liberated by freezing droplets per unit length of the cylinder is

$$Q_1 = 2R V w [L_f + c_w(T_o - T_f) + c_i(T_f - T_d)]$$

where L_f is latent heat of fusion, c_w and c_i are specific heats of water and ice, respectively, T_o , T_f , T_d are temperatures of air, freezing, and deposition, respectively. On the other hand, the rate at which heat is transferred to the environment by forced convection is

$$\begin{aligned} Q_c &= 2 \pi R h (T_d - T_o) \\ &= \pi k (T_d - T_o) \text{Nu} \end{aligned}$$

where h is the heat transfer coefficient, k is the thermal conductivity of the air,

$$Nu = f(Re, Pr)$$

is the Nusselt number, Re and Pr being Reynolds and Prandtl numbers, respectively.

The rate of heat at which heat is dissipated by evaporation is

$$\begin{aligned} Q_e &= 2 \pi R h_D (\rho_d - \rho_o) \\ &= \pi D L_V (\rho_d - \rho_o) Sh \end{aligned}$$

where h_D is the mass transfer coefficient, L_V is the latent heat of vaporization, ρ_d and ρ_o are vapour concentration at the deposit surface and of the surrounding air, respectively, D is coefficient of diffusion,

$$Sh = f(Re, Sc)$$

is the Sherwood number, and Sc is the Schmidt number. Hence the (lumped) heat balance equation is

$$2RVE w[L_f + c_w (T_o - T_f) + c_i (T_f - T_d)] = \pi[k(T_d - T_o)Nu + DL_V(\rho_d - \rho_o)Sh]$$

provided the transfer of heat by radiation has been neglected. The above relation could be used e.g. to calculate the mean surface temperature of the deposit or the critical liquid water concentration ($T_d = 0^\circ\text{C}$) for given conditions. The

values thus obtained (based on rather over-simplified relation) could be only of informative character since no account has been taken on the temperature at which the droplets actually freeze nor the heat transfer between freezing droplets and the underlying surface.

Considering the accretion on a microscopic level, the growth rate of the ice is a function of the, so called, "interface supercooling" which is the difference between the equilibrium temperature of the ice crystal and the temperature of the interface. Heat transfer between the freezing or frozen drop is a complicated process and depends on the spreading of the drop on the ice surface which is a function of the impact speed of the drop and the temperature of previously formed deposit. There have been some experiments made, e.g. by Hallet [16] and Macklin [17] on the growth of ice in bulk supercooled water, but no measurements have been made on the growth rates of ice within supercooled droplets of size occurring in natural clouds. The spreading of droplets, conveniently expressed by a spreading factor (ratio of radius after spreading to initial radius), has been investigated by Macklin [18] and Brownscombe [19]. Recently, Macklin and Payne [20] attempted to formulate a theoretical model on the microscopic level of a deposition process associated with dry regime hailstone formation. They distinguish three main phases during which the latent heat of fusion of a freezing drop is removed; the initial freezing, the subsequent freezing

and the cooling phase. The initial freezing has been described as a period of time when a newly arrived droplet is nucleated and its temperature rises rapidly towards 0°C. The subsequent freezing is controlled partly by heat conduction into the deposit and partly by forced convection and evaporation to the environment (radiation has been neglected). When the freezing process is complete the droplet is cooled by forced convection until the initial mean temperature of the deposit is regained. Although there is some overlapping of these three phases, the total time of the heat removal has been regarded as the sum of the individual times associated with each particular phase. The time of initial freezing has been calculated using data for the growth velocities in bulk supercooled water. The time of subsequent freezing and cooling phases have been calculated using analytical formulas for non-steady state heat conduction with convection rates based more-or-less on averaged interface temperatures. As a result the rate of initial freezing has been found dominant (10^{-6} sec), compared to the subsequent freezing (10^{-4} sec), and the cooling phase (10^{-2} sec.). Surprisingly, however, the calculation by the above theory agreed remarkably with the calculation based simply on the lumped heat balance equation. This would rather suggest that the new model of Macklin and Payne can not be regarded as completely realistic, since there have been a number of simplifications and approximations, some of them of doubtful justification. For

example only radial thermal gradient has been considered, the fact that at any given instant the rate of accretion and the heat transfer rate by forced convection vary over the surface has not been taken into account, the calculation in one case has been based on experimental data of doubtful applicability, etc.

2.4 Conclusions

Based on the above discussion the following can be drawn:

- (1) Theroetical up-to-date achievements seem to be completely inadequate to predict intensity, shapes and density of ice deposition under a variety of conditions.
- (2) Experimental data for practical (design) purposes obtained so far are completely insufficient to be a safe guidance for designers.
- (3) Experimental results in many cases do not seem to be sufficient to explain the nature of the physical process involved. On the other hand, in many cases where physical mechanism of an icing process can be predicted so that a physical model can be established, there are no data on particular processes involved to support quantitative analyses.

Thus it seems that experimental research on icing should be emphasized. This, in fact, has been the basic idea leading to the FROST Tunnel design which is the subject of the next chapter.

CHAPTER III

DESIGN OF THE FROST TUNNEL

The simulation of atmospheric icing requires a freezing airstream containing supercooled water droplets of predetermined size. To simulate all possible conditions that occur in natural icing clouds, the following parameters should be controlled within an icing study facility:

- (1) Air temperature and humidity
- (2) Air speed
- (3) Air turbulence
- (4) Air pressure
- (5) Drop size and number
- (6) Drop velocity
- (7) Drop supercooling

Thus, an icing study facility is essentially a low-turbulence wind tunnel with provisions for temperature and humidity control and, in addition, with a water droplets producing system (spraying system) located within the tunnel.

Any wind tunnel design is limited by various factors. Perhaps the most important ones are funds and space available. In the case of the Frost Tunnel (Figs. 3.1 and 3.2) the strict limitation was the space; 40 x 25 x 10 ft. Having the over-all size of the tunnel thus predetermined it was

low-level turbulence requirement (large contraction ratio) which resulted in relatively small cross-sectional area of the working section (18 x 18 inches) for the basic low-speed (LO-SPEED in next) design. In this regard alternative modifications, namely, slow- and high-speed (SLO- and HI-SPEED in next) have been considered (see later).

A regular octagonal cross-sectional shape of the working section and the return circuit was selected. This is an approximation of the round cross-sectional shape which is considered as a least power absorbent one for a given cross-sectional area. Also flat sides permit fewer curved surfaces and thus reduce manufacturing difficulties.

The range of wind speed in the working section (up to 150 mph) was chosen to cover most of the conditions of ship-board icing, land-based structure icing, helicopter icing, and a current problem of arctic exploration- icing on lifting, landing, and landed aircraft.

A temperature range of room temperature down to -40°C had been originally considered. However, since the first stage of the experimental program will be carried out at higher temperatures associated particularly with ship-board icing the basic LO-SPEED design was equipped with a refrigeration unit capable of producing temperatures down to -20°C . The unit was chosen such that the capacity can be increased to attain -40°C by simply adding a second stage compressor to the existing first stage and roughly doubling

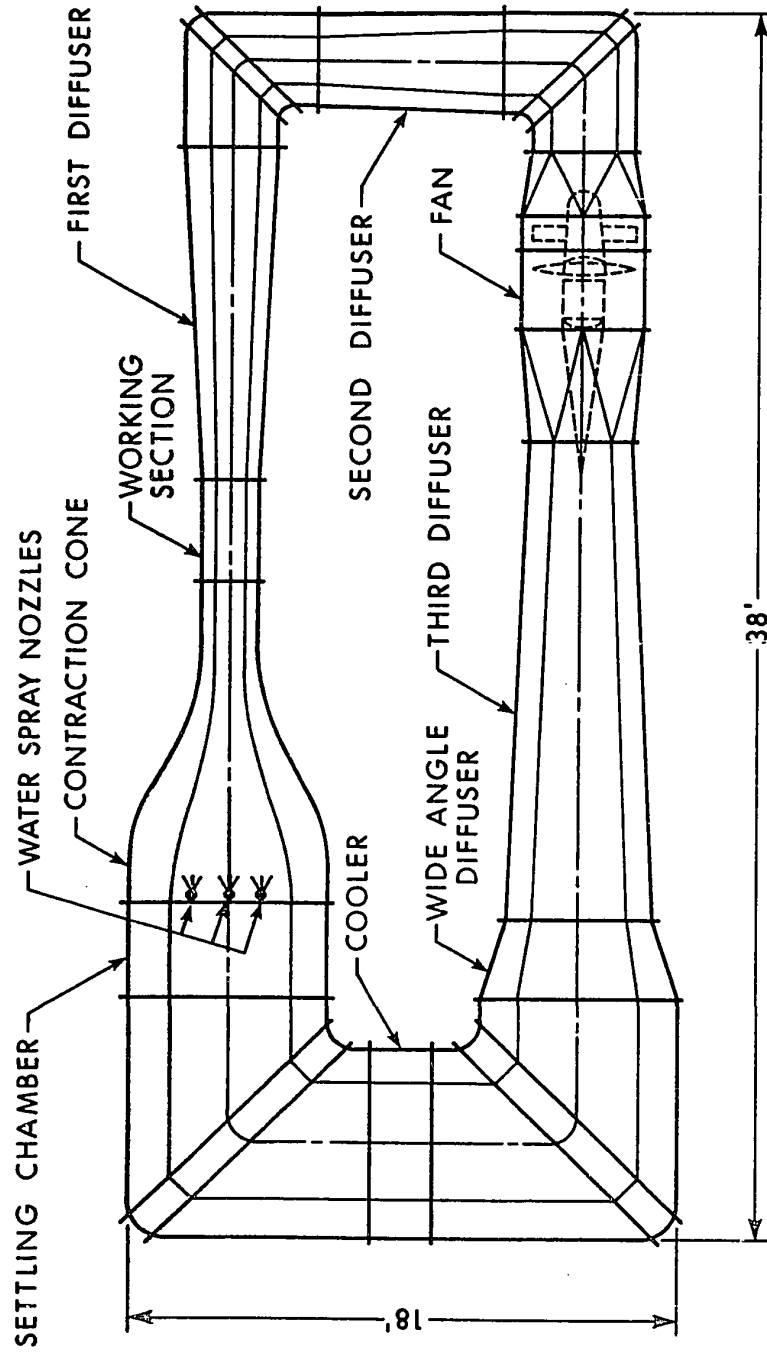


Fig. 3.1 FROST TUNNEL LAYOUT

the coils capacity (surface area).

3.1 Contraction and Working Sections

One of the most important design factors in obtaining low-level turbulence and small spatial mean velocity variations in the working section is a large contraction ratio of the contraction cone located just before the working section. The principal advantage of a large contraction is that the ratio of turbulent intensity to the mean speed will decrease through contraction cone as the mean speed increases.

The effects of contraction have been investigated theoretically by Prandtl (1933) and Taylor (1935). If U^* is the turbulent intensity defined by

$$U^* = \sqrt{\frac{1}{3} (u^{*2} + v^{*2} + w^{*2})}$$

where u^* is longitudinal, v^* and w^* are lateral root-mean-square values of velocity fluctuations, respectively, then according to Prandtl, U^* would vary as

$$\sqrt{\left(\frac{2}{3} C\right) + \left(\frac{1}{3C^2}\right)} .$$

This formula, for example, predicts increase of U^* by the factor of 3.3, approximately, for the contraction ratio of $C=16$. Thus, in this case the ratio of the turbulent intensity to the mean speed would be reduced by the factor 0.206. In

spite of the fact that this does not seem to be a substantial reduction most of the existing low-turbulence wind tunnels have the contraction ratio in the range of 10 to 20. The reasons are: firstly, Prandtl's (theoretical) formula has limitations, and secondly, a rather indirect observation, that a large contraction ratio results in a low air-speed in the settling chamber, thus permitting the installation of a number of damping screens without excessive penalty for power absorption. Thus, for the basic LO-SPEED design a contraction ratio of 16 has been used (Fig. 3.3).

In designing the contraction cone for a wind tunnel the usual design condition is that the velocity at the end of the cone, before the working section, must be fairly uniform. However, if the curvature of the wall along the flow direction is too large at certain points, local velocities at these points may exceed the uniform velocity at the end of the contraction cone. There are then regions of adverse pressure gradient and the boundary layer may separate from the wall. In the particular case of a contraction cone, the highest velocity is reached at the wall of the cone. Therefore, if the velocity at the wall is made to increase monotonically from the beginning of the cone to the end, the pressure at the wall will then be decreasing monotonically and the danger of boundary layer separation will be avoided. There have been a few methods developed to solve this problem based, essentially, on a radial expansion of an adopted axial

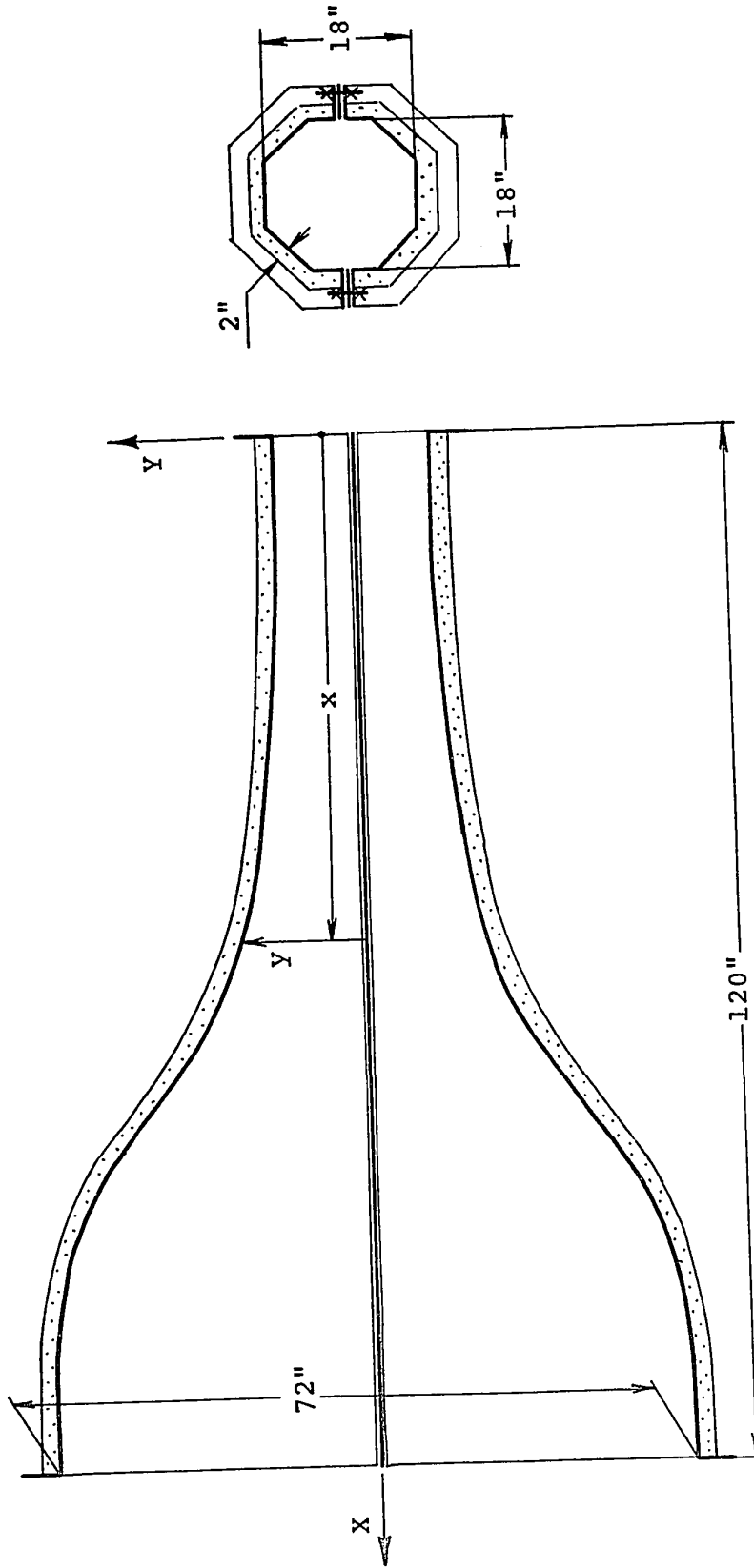


Fig. 3.3 CONTRACTION CONE

velocity distribution of a series solution of the Stokes-Beltrami differential equation. The method used here is perhaps most general, and most suitable as a practical design method and was suggested by Cohen [21]. The numerical computations were carried out using University's IBM 360/67 system. The results for LO- (as well as SLO-) design are shown in Tab. 3.1; for HI-SPEED modification in Tab. 3.2.

3.2 The Settling Chamber

The settling chamber consists of a frame and several spacers, both made of aluminium rectangular channel (see Fig. 3.4), and thus permitting installation of as many as 8 damping screens. The use of fine mesh screens in the settling chamber is to improve the flow, i.e. reduce turbulence as well as spatial (mean) velocity variation in the working section. As shown by Schubauer [22] the theoretical reduction of turbulence by n damping screens is well approximated by ratio:

$$1 / (1 + k)^{2n}$$

where k is the pressure-drop coefficient of one screen.

In our case, i.e. using 8 screens of 20-mesh size and 0.016 inch wire, the above ratio would be 0.0376. This would, for example, mean that if we have turbulence as high as 0.5% without screens (for comparison N.B.S. - U.S.A. 4 1/2 ft famous low-turbulence wind tunnel had turbulence of 0.265% without screens) we could expect turbulence reduction to

TABLE 3.1

LO- & SLO-SPEED Design:
Contraction Shape Data

X [inches]	0.00	3.42	6.84	10.25	13.67
Y [inches]	9.00	9.00	9.00	9.04	9.06
X [inches]	17.09	20.51	23.93	27.35	30.76
Y [inches]	9.10	9.15	9.23	9.33	9.48
X [inches]	34.18	37.60	41.02	44.44	47.85
Y [inches]	9.68	9.95	10.30	10.74	11.31
X [inches]	51.27	54.69	58.11	61.53	64.95
Y [inches]	12.01	12.86	13.88	15.09	16.51
X [inches]	68.36	71.78	75.20	78.62	82.04
Y [inches]	18.15	20.04	22.20	24.63	27.31
X [inches]	85.45	88.87	92.29	95.71	99.13
Y [inches]	30.07	32.55	34.29	35.21	35.60
X [inches]	102.54	105.96	108.00	120.00	
Y [inches]	35.80	36.00	36.00	36.00	

TABLE 3.2
 HI-SPEED Design:
 Contraction Shape Data

x (inches)	0.00	3.42	6.84	10.25	13.67
y (inches)	5.00	5.00	5.00	5.03	5.05
x (inches)	17.09	20.51	23.93	27.35	30.76
y (inches)	5.09	5.16	5.24	5.35	5.49
x (inches)	34.18	37.60	41.02	44.44	47.85
y (inches)	5.61	5.78	6.01	6.30	6.42
x (inches)	51.27	54.69	58.11	61.53	64.95
y (inches)	6.63	6.90	7.09	7.37	7.61
x (inches)	68.36	71.78	75.20	78.62	82.04
y (inches)	7.93	8.24	8.59	8.97	9.52
x (inches)	85.45	88.87	92.29	95.71	99.13
y (inches)	10.17	10.95	11.88	13.01	15.83
x (inches)	102.54	105.96	109.38	112.80	116.22
y (inches)	17.07	20.02	22.06	24.09	26.08
x (inches)	119.64	123.08	126.50	129.92	133.34
y (inches)	27.76	29.07	30.15	31.13	32.10
x (inches)	136.76	140.18	143.60	147.02	150.44
y (inches)	33.08	33.71	34.31	34.79	35.10
x (inches)	153.86	157.28	160.70	164.12	167.54
y (inches)	35.42	35.73	35.88	35.95	36.00
x (inches)	170.96	174.38	177.80	180.00	
y (inches)	36.00	36.00	36.00	36.00	

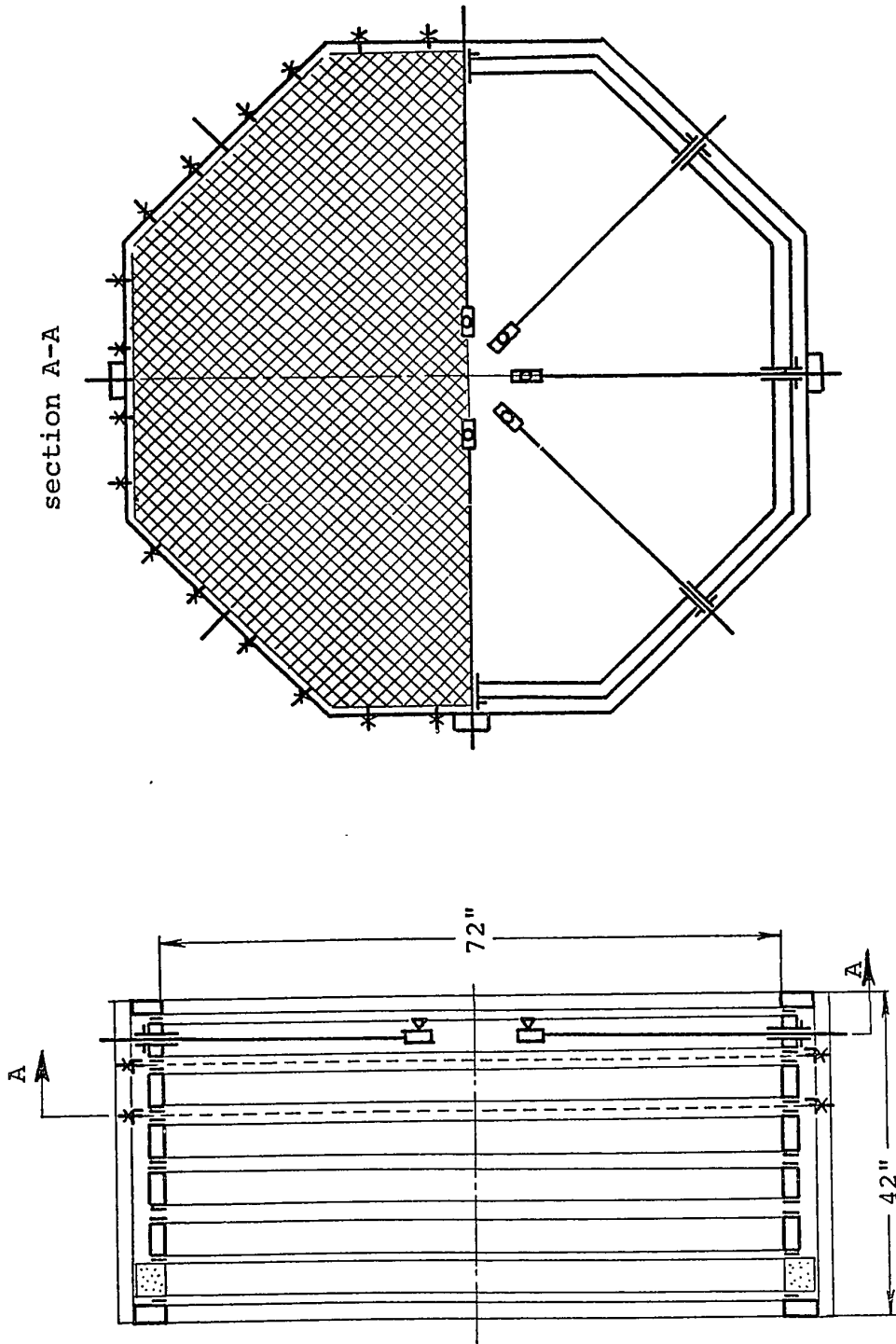


Fig. 3.4 SETTLING CHAMBER

value of 0.019% which is, indeed, a tremendous reduction - far beyond actual needs. It is common knowledge that 0.1% turbulence or less is sufficient for any laminar aerodynamic experimentation in wind tunnels and has no further effect on transition. However, the experimental verification of the theoretical formula shows that particularly for $n > 5$ the formula is less accurate and predicts a bigger reduction than has been observed.

3.3 Diffusers

Since the power losses in a wind tunnel vary with the cube of the air-speed, it is desirable to increase the cross-sectional area of the return passage as quickly as possible. The rate of the area increase is limited by the amount of expansion which the boundary layer will stand without separating from the wall. Townsend [23] has shown that a turbulent boundary layer can survive unlimited retardation without separation if the velocity varies more slowly than a certain power of the distance from the boundary layer origin. This power depends on the Reynolds number but is always more positive than $-1/3$. The position at which the actual power law index falls below $-1/3$ depends on the diffuser angle and the thickness of the boundary layer at entry, and in the present state of boundary layer theory precise design rules do not exist. Based on experimental observations, however, a diffuser of 5 to 7 degs of total included angle will yield

satisfactory flow if relatively small area ratios are used (up to 3) [24]. On the other hand, there are methods permitting use of far larger cross-sectional area expansions, perhaps up to 50-60 degs of total included angle: these methods are based on boundary layer control schemes such as suction and blowing, the use of splitters, vortex generators, windmills, screens etc. Unfortunately, the situation regarding design methods or experimental data available on these methods is even worse. Perhaps the most promising method of boundary layer control by suction seems to involve too many technical complications.

In designing the diffusers for the FROST Tunnel the problem was to enlarge the size of the working section (1.5 x 1.5 ft.) to the size of the settling chamber (6 x 6 ft.) within the length of the tunnel available (36 ft.). There were three possible locations where the diverging section could be used. The first one, located just after working section is 10 ft. long and is the location of the first diffuser using the following parameters:

Area ratio: 2.8

Total angle: $5^{\circ}40'$

The second diffuser, located between the first and second corner is 8' - 5" long and has parameters:

Area ratio: 1.3

Total angle: $5^{\circ}10'$

The third diffuser, located just downstream of the fan, is 15' - 8" long and has parameters:

Area ratio: 2.25

Total angle: 6°5'

The fourth, wide angle diffuser, is next (downstream) of the third diffuser. The parameters are:

Area ratio: 1.5

Total angle: 28°30'

It is clear from the above parameters and Fig. 3.2 that the first three diffusers are of conventional design i.e. linearly expanding ducts with parameters within recommended values. In fact first two diffusers must be of conventional design since heavy icing may occur there so that other design alternatives seem to be unacceptable. The reasons for the conventional design of the third diffuser have been:

(1) Boundary layer control by suction and blowing would present great complications (e.g. additional cooling system for "auxiliary air") and will be costly.

(2) It is not known precisely how and when the use of splitters, windmills, screens, and vortex generators is appropriate. It is a matter of trial and error for any particular situation. Moreover, in spite of the fact that the diffuser parameters are in "safe region," the technology of manufacturing process may cause limitations (e.g. "wavy walls" which is quite possible for such a long piece of duct made of fibreglass). In such cases the above means could be

used to improve performance of the diffuser.

The reason for the particular design of the fourth (wide-angle) diffuser was space limitation. However, as soon as there is more lab space for the FROST Tunnel it will be replaced by another conventional diffuser of the parameters:

Area ratio: 2.3

Total angle: $6^{\circ}10'$

which will actually be a continuation of the third diffuser with the same parameters.

There are two reasons for this replacement:

(1) A wide-angle diffuser consumes more energy (because of screens - discussed below) than an "equivalent" conventional one

(2) For FROST Tunnel modifications (see Sec. 3.6) there is a requirement for additional length-space of the tunnel.

The wide-angle diffuser devised in the first place is a useful experiment. As stressed before, no reliable design data are available presently. However, Bradshaw and Pankhurst of N.P.L. [25] (perhaps the most qualified experts on wind tunnel design), say: "A 45° equivalent cone with about three screens fitted in intervals has been found to maintain satisfactory flow with an area ratio of It is doubtful whether the flow in wide-angle diffusers is entirely free of separations, but minor regions of separated flow do not seem to produce unsteadiness in the working section." Thus, three screens of 20 wire size and 16 inches wire diameter (one at

the beginning, middle and end, respectively) were used.

3.4 The Corners

The cost and limited space available in most wind tunnels usually requires the design of abrupt corners with losses kept to the minimum by means of proper turning vanes. Corner vane camber lines can be designed by cascade theory to approximate to any given camber line in an infinite stream, "but in practice a circular arc camber, subtending an angle slightly less than 90° is adequate" - as experienced by Bradshaw and Pankhurst [25]. It has also been found that sheet metal vanes are adequate, and may even be more efficient than streamlined vanes since excessively thick vanes in a cascade cause blockage and the resulting adverse pressure gradients over the trailing edges of the vanes will cause rapid boundary-layer growth which may result in separation and loss of efficiency. Thus a gap/chord ratio of $1/4$, a leading edge angle of $4-5^\circ$, and trailing edge of 0° appear to give the best performance [25]. In the actual design the above rules were followed precisely. The frame and turning vanes were made of aluminium sheet material welded together.

3.5 The Fan and Refrigeration

The calculation of power and heat losses which resulted in the particular choice of fan and refrigeration unit respectively, are presented in appendix.

3.6 FROST Tunnel Modifications

As mentioned before, the SLO- and HI-SPEED modifications of the basic LO-SPEED design have been considered for future experimentation.

The SLO-SPEED modification (Fig. 2.5) is simply a rearrangement of two major (one existing) sections of the tunnel, namely, the contraction cone and the working section. Thus a 6 by 6 ft. and 11 ft. long working section (to be manufactured) will be located just after (downstream) the settling chamber whereas the existing contraction cone will be located after the working section. The principal advantage of this modification is that larger-scale model tests could be performed, however, in a lower speed range (0 - 15 mph).

The HI-SPEED modification (Fig. 2.5), as compared to the basic LO-SPEED design, differs in the contraction section, the size of the working section (10 by 10 inches) and the speed range of up to 450 mph (estimated). This will enlarge the extent of experimental studies to include aircraft icing. For the modification, a contraction cone of ratio 52 and of length 15 ft., a short straight-walled diffuser (length 7 ft., see Fig. 2.5) and a new working section would have to be manufactured.

3.7 The Spraying System. The purpose of the spraying system is to produce a certain spectrum of droplet sizes of spatially uniform distribution. Each spray nozzle must be capable of sufficient water flow to satisfy maximum liquid-water

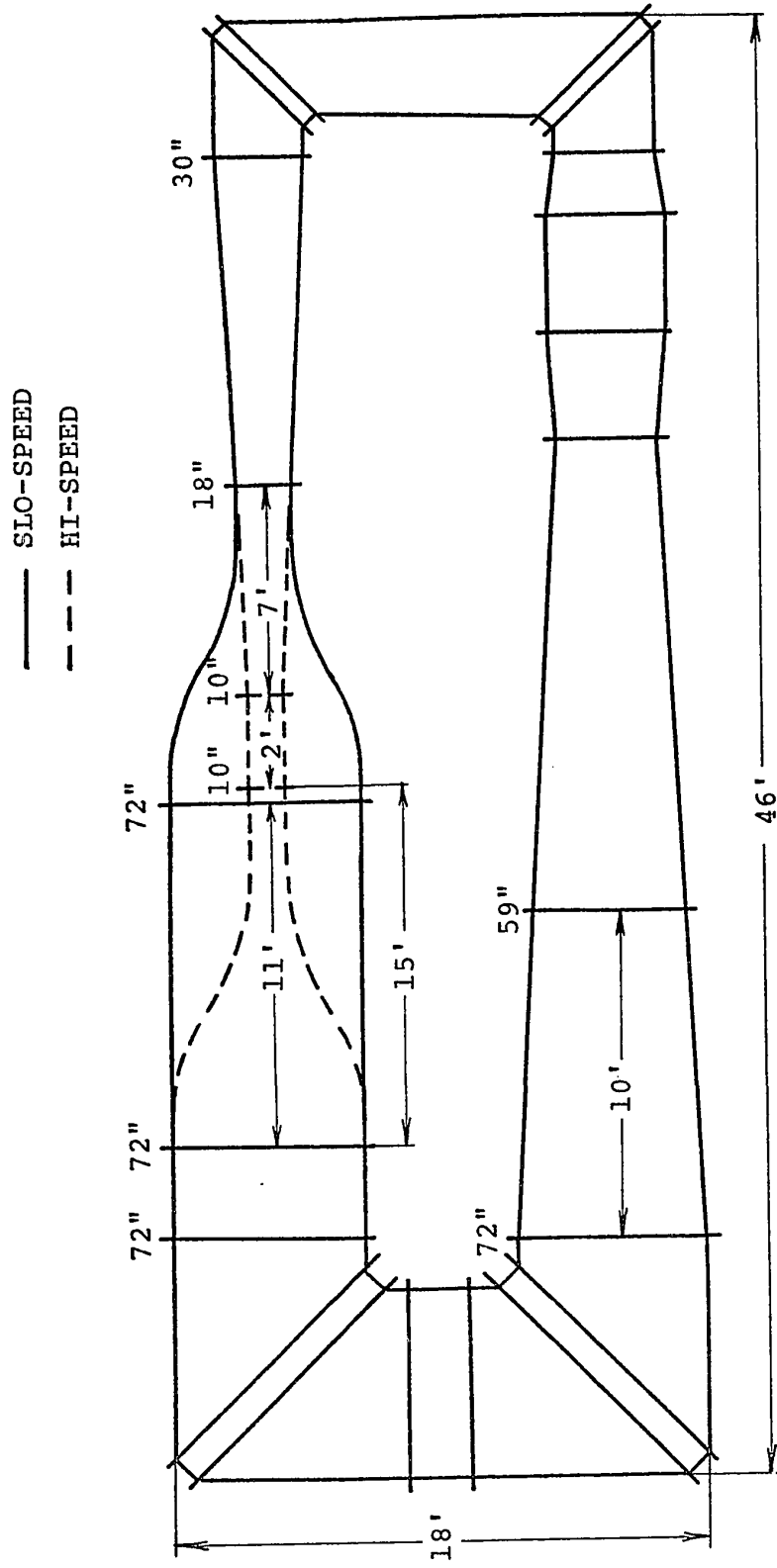


Fig. 3.5 FROST TUNNEL LAYOUT : SLO- & HI-SPEED MODIFICATIONS

content requirement which was chosen to be 60 g/s. This represents liquid-water concentration of about 5 g/m^3 at maximum speed (150 mph) and would cover perhaps all possible icing situations. For illustration, liquid-water content up to 1 g/m^3 , approximately, occurs in high altitude clouds. The range of drop sizes and their distribution in clouds and sea sprays (drop size of 10 microns up to 1 cm) is so wide that it is impossible to cover the whole range by means of one nozzle design. Therefore, standard existing nozzles, capable of producing droplets of 10 to 200 microns, approximately, were chosen for the first stage of experimentation. In particular, a "Spray Set-Up No. 11" consisting of the "Fluid Nozzle 205" and "Air Nozzle 67147" designed and manufactured by Spraying System Co., Bellwood, Illinois, U.S.A. meets the above requirements. Considering the spray area coverage of one nozzle, an array of 5 nozzles was devised to cover uniformly the whole cross-sectional area of the working section. Moreover, enough flexibility in the design (the position and angle of inclination of the nozzles with respect to the stream can be changed) were left to overcome eventual non-uniformities in the spatial spray distribution. The design of the whole system is illustrated in Fig. 3.6. The air entering the air nozzle is preheated thus preventing freeze-out conditions at the water nozzle and the water circuit is equipped with a cooling unit to control the water temperature (drop supercooling).

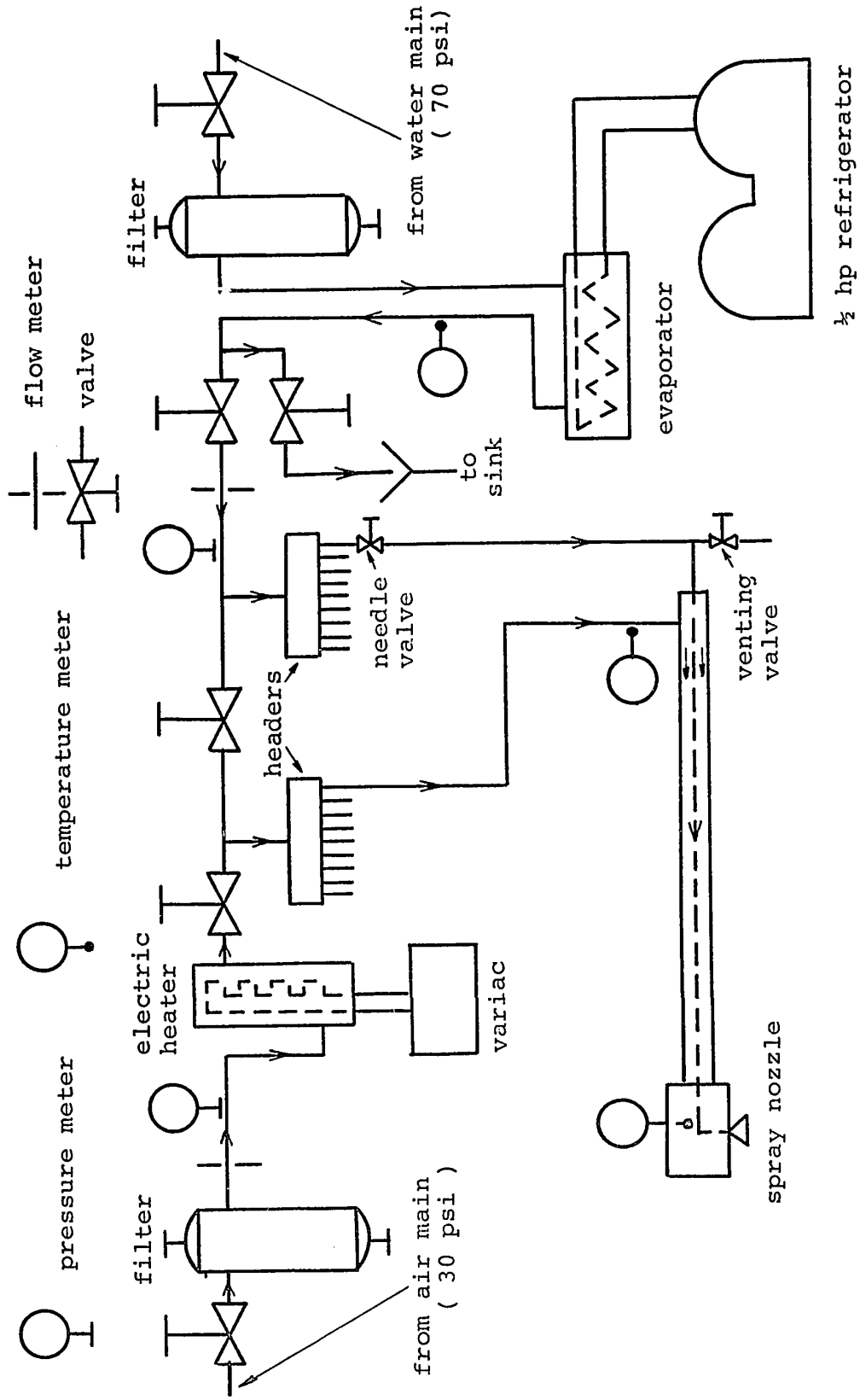


Fig. 3.6 SPRAYING SYSTEM

Since the first stage of experimental studies will be devoted to icing resulting from presence of water droplets in atmosphere which exists naturally, under saturated conditions, no provisions were made for the humidity control. The humidity control, however, will be necessary if "hoarfrost" ice deposition (hoarfrost is a deposit of interlocking ice crystals formed by direct sublimation of water vapours on objects) is studied. Such a control would consist of a fine spraying system and moisture removal system governed by a humidity (dew point) sensor: its design is being carried out presently.

CHAPTER IV
INSTRUMENTATION, CALIBRATION, AND
PRELIMINARY EXPERIMENT

A water-droplet-laden airstream is essentially defined when its velocity and temperature variation, the droplet size distribution and its spatial uniformity, and the liquid-water content, along with air turbulence is known.

4.1 Velocity Measurement

The wind speed was measured by means of standard pitot-static tube. A pitot-static tube reads the dynamic pressure, i.e. the difference between the total and static pressure, which by definition is

$$q = \frac{1}{2} \rho v^2$$

where v is the airspeed, ρ is the density of air evaluated at temperature and pressure of the working section. The pressure difference was measured by an inclined fluid manometer. Usual corrections, namely, the tip and stem errors have been taken into account.

For the velocity survey, the pitot-static tube was moved around and across the working section and the dynamic pressure was measured by a micromonometer. The variation of velocity in the working range of the tunnel has

been found to be less than 0.2% from the mean at 90 mph when 6 dumping screens (of 20 mesh-size and 0.016 inches wire dia.) were in the settling chamber.

4.2 Temperature Measurement

It is difficult to measure temperature in an icing cloud and a satisfactory (direct) method has not yet been developed. Perhaps the best method available presently is to measure temperature in a low velocity water-and ice-free region and calculate temperature in the working section on the basis of the subsequent flow changes being expected; particularly, heating due to spray. This has the evident disadvantage that the actual test temperature could only be calculated when the amount of spray frozen is known, i.e. usually at the end of an experiment. However, these differences are not substantial and can be readily predicted. Hence the temperature was measured in the settling chamber just upstream of the spray nozzles by means of 10 copper-constantine thermocouples; two of them being located at the centreline of the tunnel, the others circumferentially distributed about 5 inches from the tunnel walls and all at the same cross-sectional plane of the settling chamber. The thermocouples, equipped with cold junctions, were connected to a microvoltmeter through a switching unit. In calibration of the thermocouples, it was found (using a fine potentiometer and a fine mercury thermometer) that voltages read by the

microvoltmeter followed very closely the standard (wire) calibration curve.

The temperature variation across the stream was measured by a special probe consisting of five series - connected thermocouples. As a result, a temperature variation of less than 0.10°C was observed at -15°C of air temperature, and at 90 mph.

4.3 Turbulence Measurement

A constant temperature T.S.I. (Thermo System Inc.) hot wire anemometer (model no. 1051-2) equipped with a single hot film sensor and a rms voltmeter were used to measure the turbulence intensity. Because of the availability of only a single sensor, the turbulence intensity in the mean flow direction alone (u^*/U) was measured. The probe was located in the working section at the centerline of the tunnel. The turbulence intensity was measured at room temperature (68°F) at 20, 50, 90, and 140 mph. Its value has been found to be within 0.03 - 0.08%, the latter value corresponding to 140 mph.

4.4 Droplet Size Distribution Measurement

An oiled-slide technique [26] was used to determine droplet size distribution in clouds. The instrument (Fig. 4.1) consists of a glass slide "A" covered with a suitable oil which, while being exposed for a short time in a droplet-laden

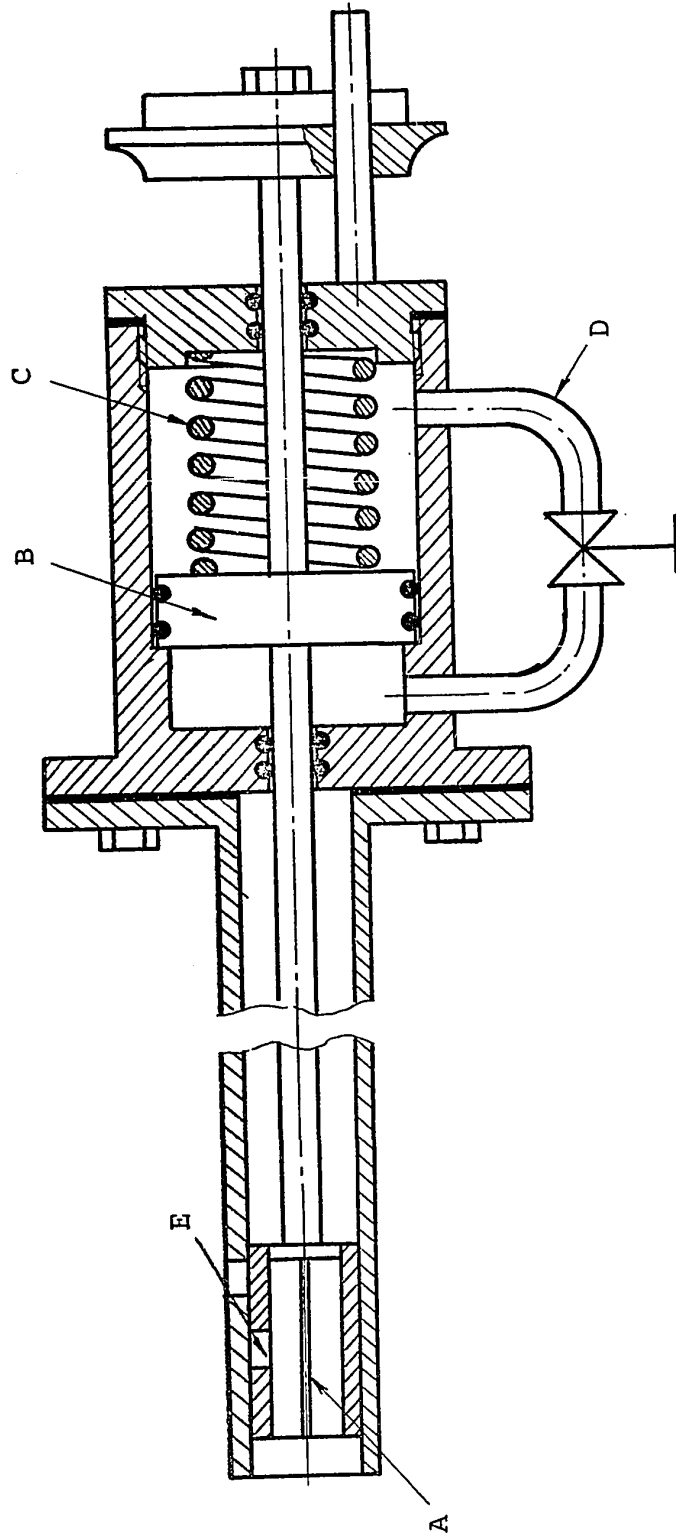


Fig. 4.1 DROPLET SAMPLER

airstream, collects droplets and is then photographed through a microscope. In taking droplet samples, the most important factor to consider is the exposure time of the oiled slide in a cloud. If it is too short the number of droplets collected is insufficient to represent the variety of sizes. If it is too long, too many droplets are collected, thus increasing probability of coalescence which leads to an error in the observation. The proper exposure time, depending on the size, number density, and the velocity of impact, has been therefore determined by trial for each condition. The timing device of the instrument designed and used is based on the function of a hydraulic damper; the motion of the piston "B" initiated by a spring "C" is controlled by the rate of by-passing of a liquid (oil) through a line "D" connecting two sides of the piston inside the cylinder. An oiled-slide carrier connected to the piston has a circular opening "E" which moves axially inside a cylindrical housing with a similar opening. When these two openings coincide droplets are allowed to impinge on the oiled surface. The slide must be covered by a special oil which retards evaporation of droplets sufficiently long to have a photomicrograph taken. Golitzine [26] who examined a number of oils and lubricants found that the property of retarding evaporation does not depend on the viscosity of oil nor on the additives alone. However, he found that "Shell Spirax 250" gave the most satisfactory results. Unfortunately,

since this oil is not available on the market presently, alternative choices with the properties closest to Shell Spirax 250 were made. "Shell Spirax 140 E.P." and Shell Omala 85" were examined with the latter giving better results (as to the retarding evaporation) and thus being predominantly used.

The photomicrographs were taken using Leitz-Wetzlar (Germany) microscope and Miranda (1.8/50 mm) camera loaded with Kodak Plus - X (125 ASA) film, the exposure time being 1/8 sec. The prints were enlarged on 6 x 8 inches plates thus giving an over-all magnification of about 250. A semiautomatic particle-size analyser, developed and manufactured by the Research Institute of Chemical Equipment, Prague, Czechoslovakia, was used to determine size-distribution curves. The analyzer enables up to 1000 droplets to be examined in one hour.

4.5 The Liquid-Water Content Measurement

The nozzle water flow rate was used to determine the liquid-water content of a simulated cloud. The flow rate was measured by a mean calibrated flow-nozzle located before the header (Fig. 3.2) in the spraying system water line. However, since under some conditions, an unknown amount of water freezes on the tunnel walls and in addition some water may be lost by evaporation, a supplementary measurement based on the cloud-drop microphotography was

attempted.

Ideally, for a given water flow rate and air-speed, i.e. for a given liquid-water content, (mean) drop size variations could have been obtained by changing the nozzle air pressure. As experienced, however, varying of the nozzle air pressure, the nozzle water flow rate and particularly the airspeed often led to a change of the spray area coverage in the working section. Thus for every set of parameters, the spray area coverage had to be checked to get an accurate value of the liquid-water content.

4.6 The Experiment

The experiment was designed to check the ability of the Frost Tunnel to produce conditions in which icing under both wet and dry regimes can be studied.

A hollow circular cylinder; 2 inches in diameter and of 1/8 inch. wall thickness, fixed vertically in the working section, was selected as the subject of present icing study.

For chosen conditions; wind speed of 46 mph (40 knots), air temperature of -10°C , and (mean) drop size of 70 microns, the calculation based on the lumped heat balance equation showed that the critical liquid-water content of the simulated cloud would be of the order of $1\text{g}/\text{m}^3$. However, after a few trial runs it became apparent that the actual critical liquid-water content for the above conditions would be higher; $3\text{g}/\text{m}^3$ approximately. Thus for run no. 1 (identical to

"A4" [2]), intended to give spray glaze deposit (wet regime), a value of 4g/m^3 was selected.

After a few failures to obtain crystalline rime deposit (dry regime) - essentially because of non-uniformities of the spray spatial distribution in the working section - a "good" test (identical to "A3" [2]), resulting in an intermediate (near critical) ice deposit, was completed when the (mean) drop size and the cloud liquid-water content were altered to 30 microns and 4.5g/m^3 , respectively.

4.7 Test Results and Discussion

The test results are shown in Tab. 4.1, the front view photographs taken after 30 mins. of deposition are on Fig. 4.2 and Fig. 4.3, and for the photomicrographs of the spray see Figs. 4.4 and 4.5. In analyzing the microphotographs, it has been found that the particle sizes are represented by dark circles whereas the lighter rings around them are results of light diffraction and dispersion.

As expected run 1 resulted in a spongy glaze deposit (Fig. 4.3). The deposit is of a "mushroom-type" commonly experienced under over-critical conditions; the stagnation region of virtually 100% local collection efficiency was "warmed up" by water more intensively than any other region so that actual ice formulation went sidewise horizontally thus widening the frontal area of the deposit. As a result the mass icing efficiency [27] defined by ratio

TABLE 4.1

TEST RESULTS

Run Number	1	2
Liquid-Water Content [g/cm ³]	4.0	4.5
Air Temperature [°C]	-9	-10
Wind Speed [mph]	46	46
Mean Drop Diameter [microns]	75	30
Collection Efficiency [%]	Initial 90	70
	Final (estimated)	210
Mass Icing Efficiency [%]	109	12

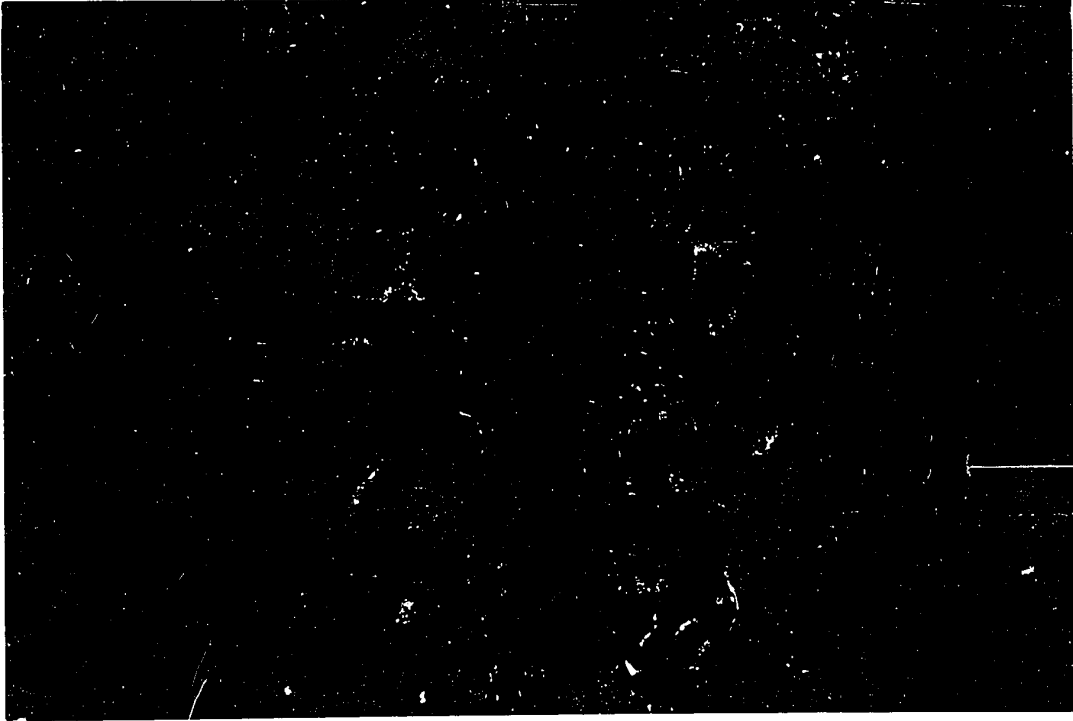


Fig. 4.2 RUN No.1: ICE DEPOSIT AFTER 30 MIN.

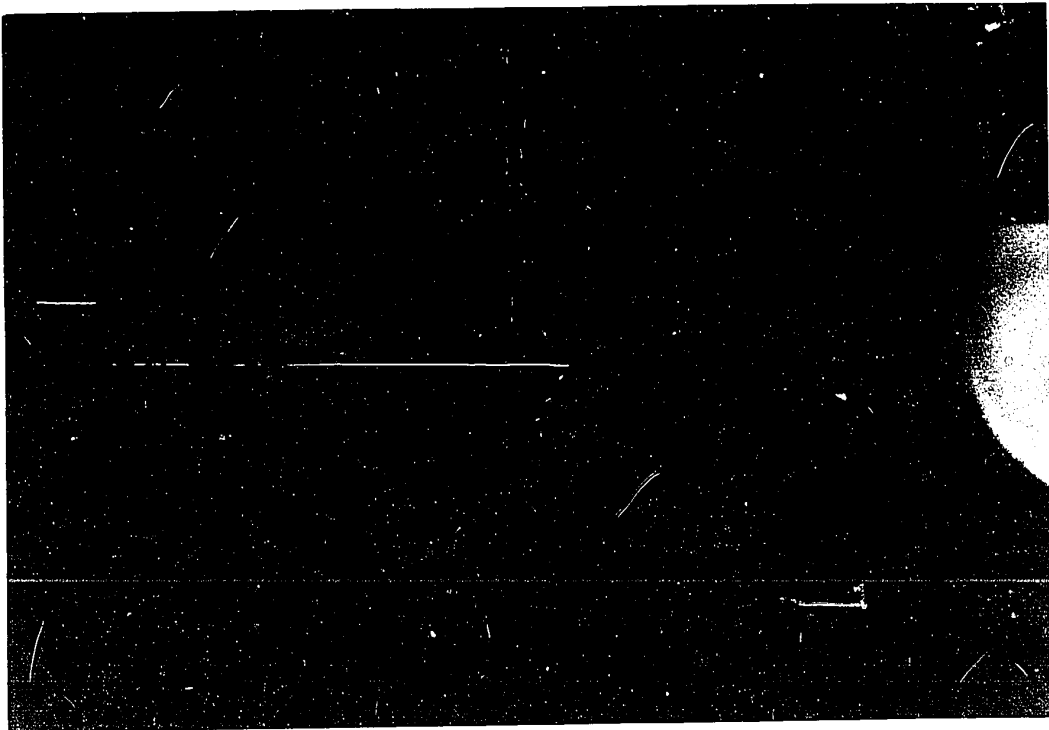


Fig. 4.3 RUN No.2: ICE DEPOSIT AFTER 30 MIN.

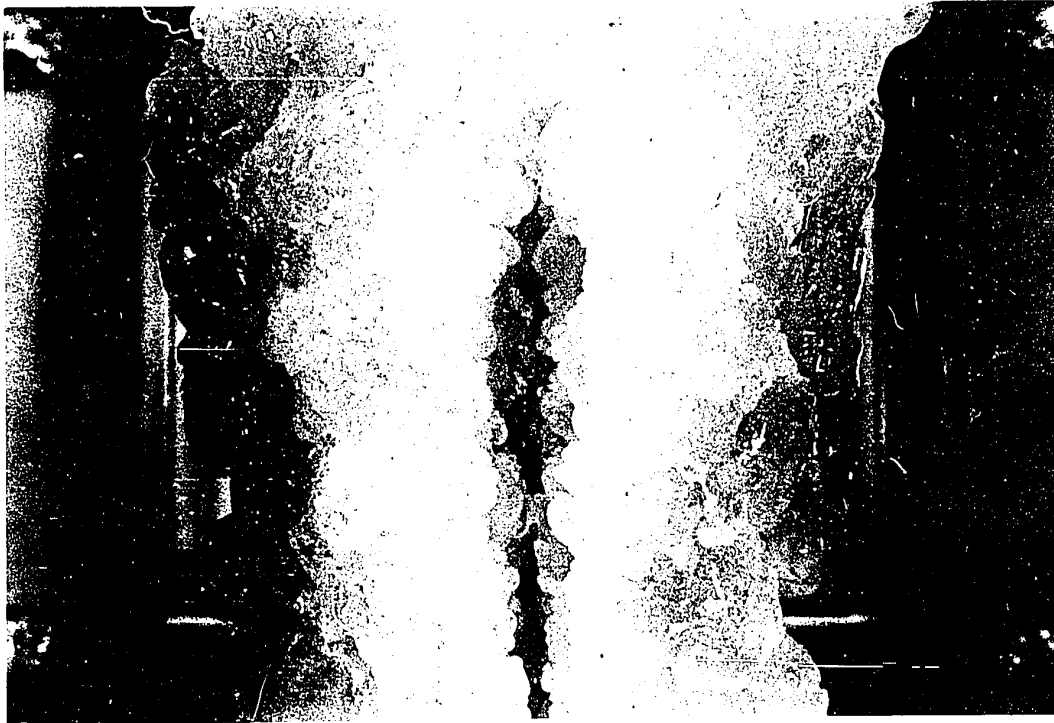


Fig. 4.2 RUN No.1: ICE DEPOSIT AFTER 30 MIN.



Fig. 4.3 RUN No.2: ICE DEPOSIT AFTER 30 MIN.



Fig. 4.4 RUN No.1: MICROPHOTOGRAPH OF A SPRAY SAMPLE (150 x)

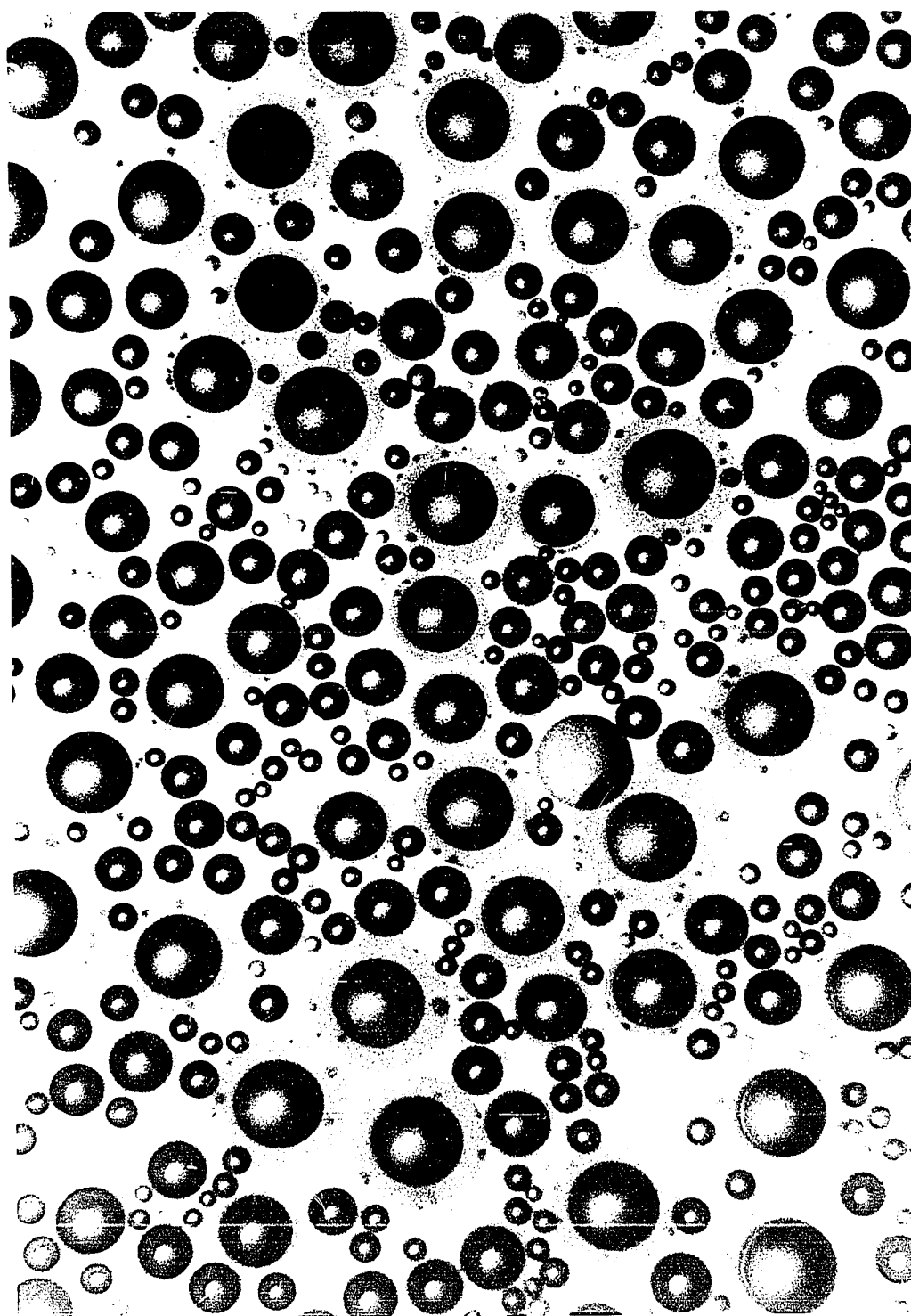


Fig. 4.4 RUN No.1: MICROPHOTOGRAPH OF A SPRAY SAMPLE (150 X)

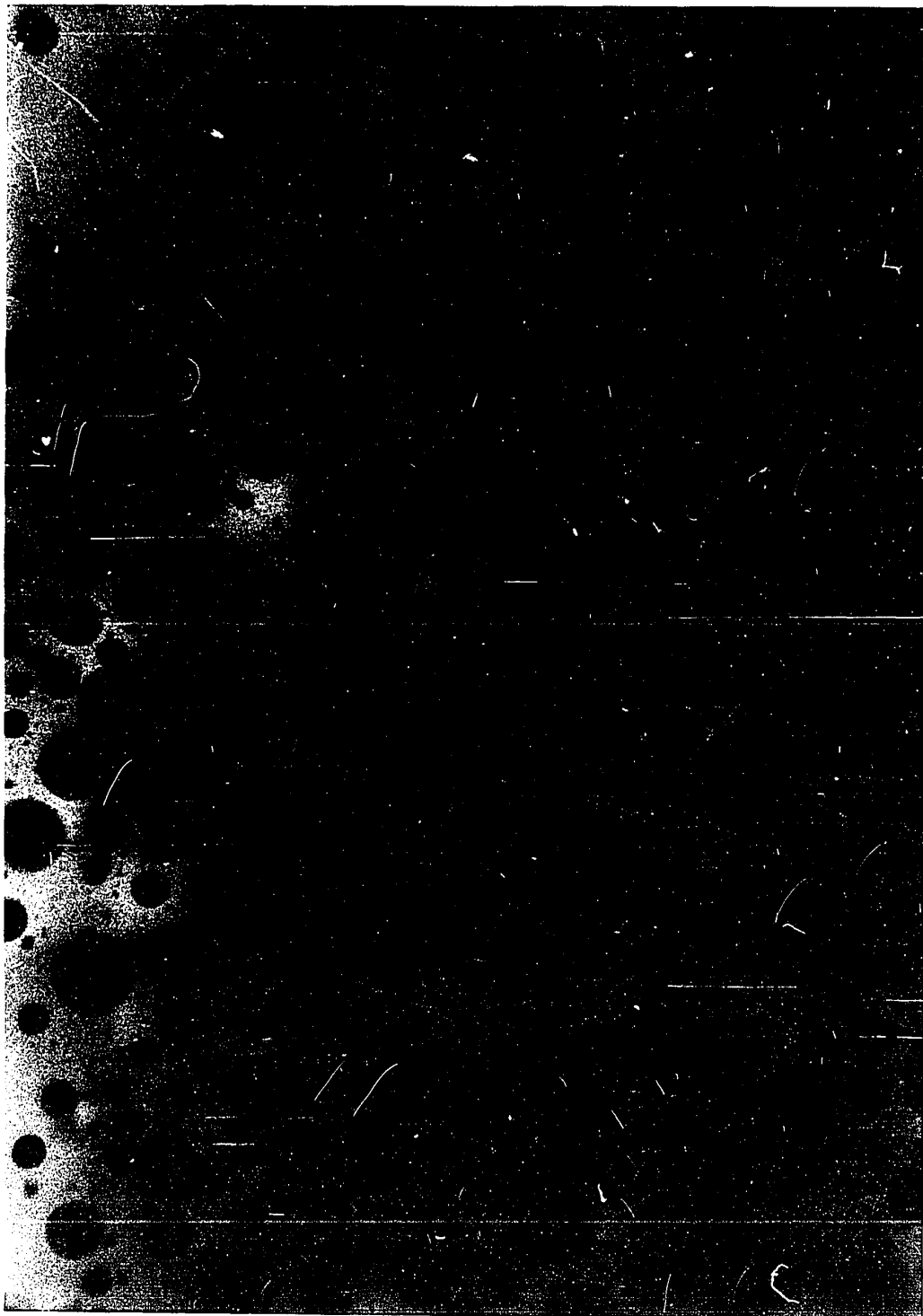


Fig. 4.5 RUN No.2: MICROPHOTOGRAPH OF A SPRAY SAMPLE (150 x)

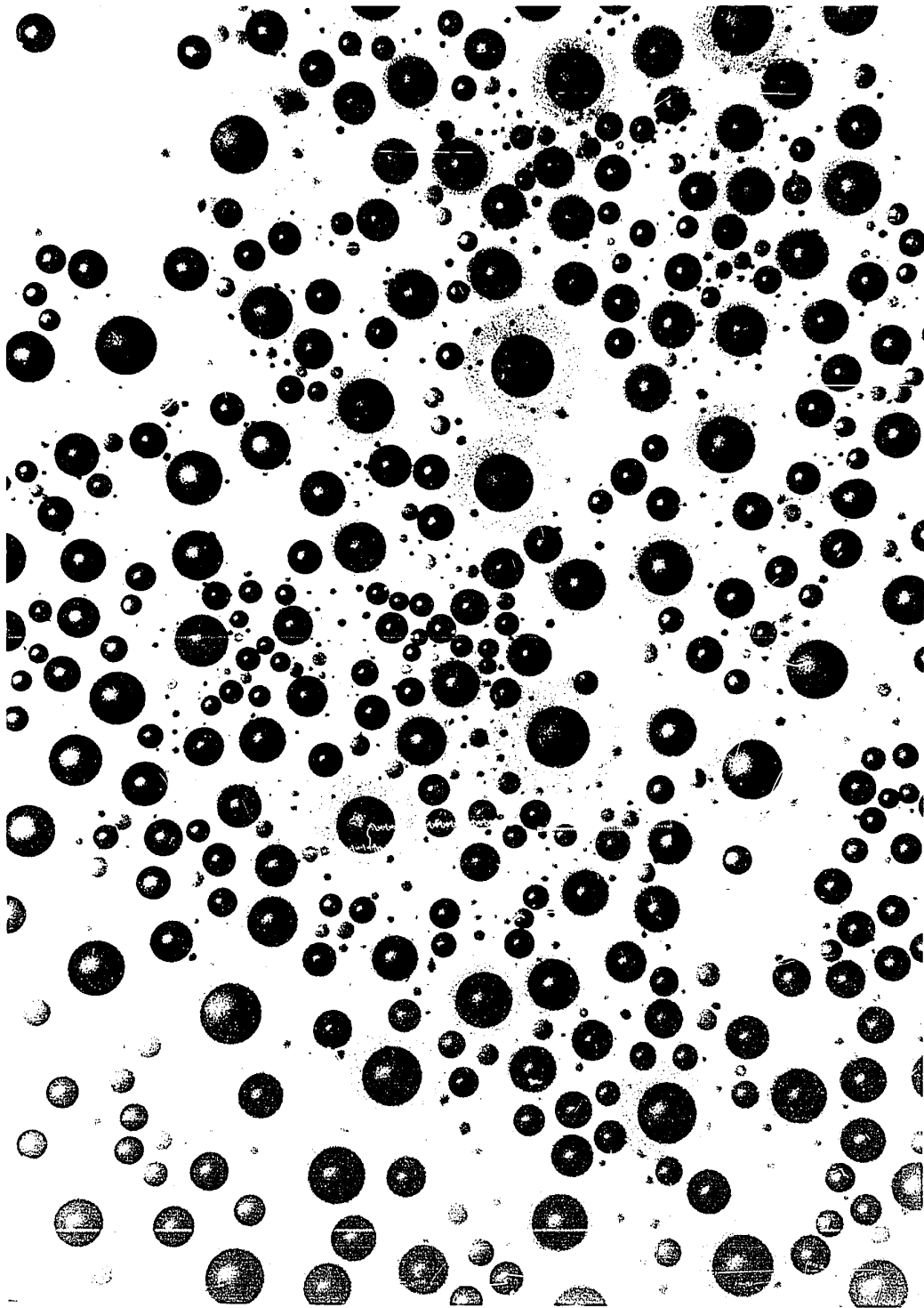


Fig. 4.5 RUN NO. 2: MICROPHOTOGRAPH OF A SPRAY SAMPLE (150 X)

weight of ice actually deposited in 1/2 hour
weight of water spray that would deposit on projected surface
in 1/2 hour

was relatively high (109%).

Run No. 2, a compact glaze formation in and around the stagnation region with crystalline rime deposit at sides of the cylinder (Fig. 4.4), was found to have a surprisingly low mass icing efficiency (12%). This fact brought up certain doubt about proper measurement of spray characteristics; in particular, the liquid-water content of the cloud. A supplementary measurement revealed that the corrected value of the cloud liquid-water content was higher than it was before and even higher than that of run No. 1. In fact the flowmeter read the same value but the spray area coverage was smaller.

Unfortunately, in both cases a check through microphotography was not possible since the timing device of the sampler did not function accurately. This "worsened" the situation (the liquid water content was expected to be lower) since one would expect that a heavier spray would result in a heavier ice deposit. On the other hand, because of different (mean) drop size, the initial collection efficiency of run No. 2 (70%) was less than that of run No. 1 (90%). Moreover, while the collection efficiency of run No. 2 was virtually not increasing during the experiment, the collection efficiency of run No. 1 was rapidly increasing and at the end

of the run was estimated to be about 210%. It is doubtful, however, whether one order-of-magnitude drop in the mass icing efficiency could be justified by the foregoing observation. Thus, it would appear that the actual liquid-water content of the simulated clouds was not precisely known so that the present technique of its measurement was not adequate.

CHAPTER V

CONCLUSIONS AND RECOMMENDATIONS

5.1 Conclusions

The calibration as well as preliminary tests revealed the following:

(1) The FROST Tunnel is capable of working in the range of wind speeds and air temperatures for which it was designed (up to 150 mph and down to -20°C , respectively). Moreover, the range of wind speed could be increased (up to 450 mph) and larger scale models could be tested (modifications).

(2) The airstream in the working section represents a fine uniform "jet" with spatial velocity variation less than 0.2%, turbulence intensity level in the mean flow direction in the range of 0.03 to 0.08%, and spatial temperature variation less than 0.10°C .

(3) The spraying system is capable of producing a cloud liquid-water content of 60g/sec. or more. However, it is limited in range, depending on the wind speed and drop size.

The cooling system built into the spray water line (water temperature control) did not function satisfactorily since the evaporative exchanger (Fig. 3.6) often froze. Also temperature and flow rate of the air flowing through a

line surrounding the water line were not high enough to prevent freezing-up conditions at the water nozzle. It was found that the water did not freeze in the water line but in the nozzle body itself.

5.2 Recommendations

Based on the discussion in the previous section and Chapter IV the following alterations in the design, instrumentation, and methods used are suggested.

(1) Spraying System:

To improve the spatial uniformity of the spray in the working section an array of 9 nozzles instead of 5 nozzles should be used.

The evaporation exchanger of the water cooling system should be redesigned or an alternative system (Fig. 5.1) could be considered. This consists of a single U-tube (one for each nozzle) immersed into the main air-stream so that the water temperature can be simply controlled by changing of depth of the U-tube insertion.

To prevent "freeze-up" conditions at the water nozzles single electrical heaters may be installed within the nozzle bodies.

(2) For particle-size and distribution measurement, although the oiled-slide technique gave satisfactory results, there is a need for another (checking) method. In recent years there have been a number of developments (e.g. based

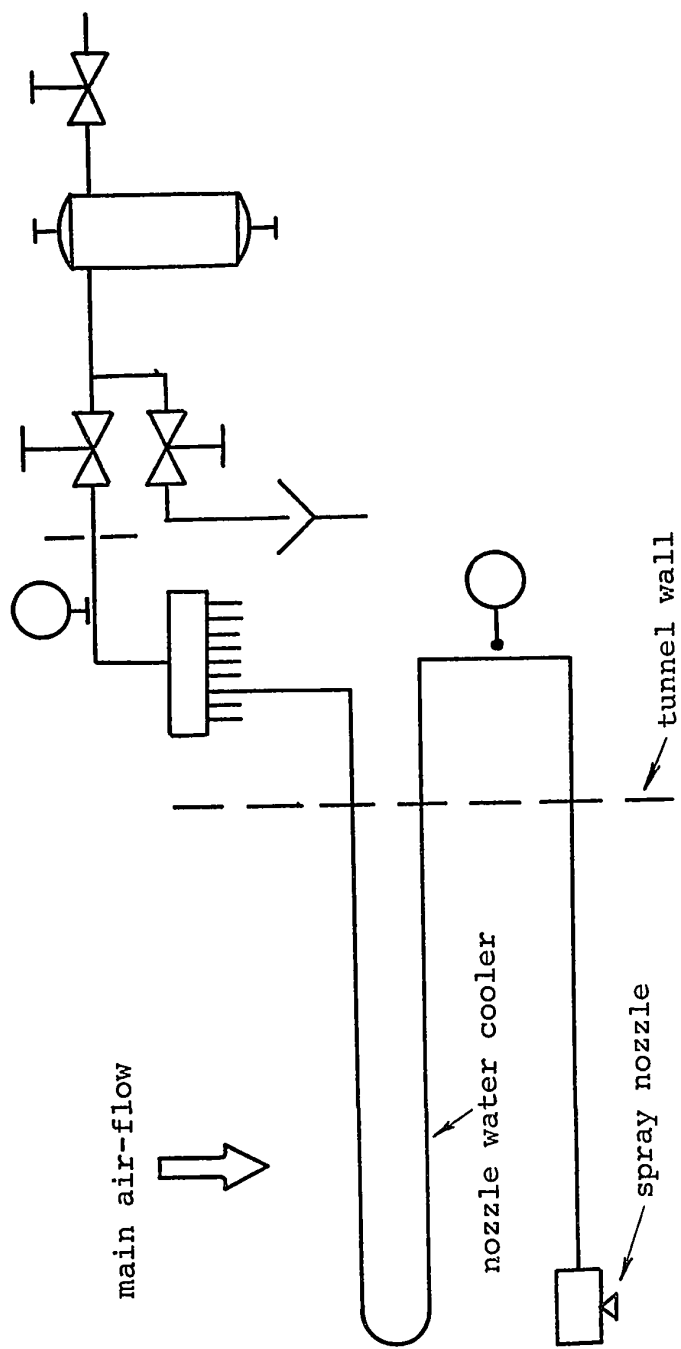


Fig. 5.1 ALTERNATIVE NOZZLE-WATER TEMPERATURE CONTROL ARRANGEMENT

on measurement of the transmission of infrared light through a cloud and other light-scattered techniques [28]: however, their reliability is still in doubt. There are a few more established techniques such as direct cloud photography [29] and rotating multicylinder method [29], but these have several disadvantages. A determined search for other suitable techniques is being carried out presently.

(3) For liquid-water content measurement an improved timing device for the droplet sampler which would give a better adjustment of the exposure time will allow a required check through microphotography. However, since knowledge of precise values of the liquid-water content seems to be an important factor in icing cloud simulations, yet another method would be desirable. Among the possible methods, the hot wire technique - a wire heated electrically, exposed to the airstream, is cooled by impinging droplets; the magnitude of this cooling is a measure of the water content [30] - is used most widely and is recommended.

REFERENCES

REFERENCES

1. Hacker, P. T. and Dorsch, R. G., "A Summary of Meteorological Conditions Associated with Aircraft Icing and a Proposed Method of Selecting Design Criteria for Ice-Protection Equipment," N.A.C.A. Tech. Note 2569, 1951.
2. Lock, G. S. H. "Some Aspects of Ice Formation with Special Reference to the Marine Environment," Transactions of the North-East Coast Institution of Engineers and Shipbuilders - U.K. (in Press).
3. Stallabrass, J. R., "Meteorological and Oceanographic Aspects of Trawler Icing off the Canadian East Coast," The Marine Observer, Vol. 41, 1971.
4. Boyd, D. W., "High Winds and Low Temperatures Associated with Freezing Precipitation," N.R.C. Building Note No. 18, 1965.
5. Boyd, D. W., "Icing Observations 1964-65 - First Progress Report," N.R.C. Tech. Note No. 459, 1965.
6. Mossop, S. C., "The Freezing of Supercooled Water," Proc. Phys. Soc. B, Vol. 68, 1955.
7. Bigg, E. K., "The Supercooling of Water," Proc. Phys. Soc. B, Vol. 66, 1953.
8. Hoffer, T. E., "A Laboratory Investigation of Droplet Freezing," Journ. Meteor., Vol. 18, 1961.
9. Pruppacher, H. R. and Neiburger, M., "The Effect of Water Soluble Substances on the Supercooling of Water Drops," Journ. Atmos. Sc., Vol. 20, 1963.
10. Langmuir, I. and Blodgett, K. B., "A Mathematical Investigation of Water Droplet Trajectories," A.A.F. Tech. Report No. 5418, 1946.
11. Levin, L. M., Doklady A. N. SSSR, Vol. 91, 1953.
12. Fuks, N. A., "Mechanika Aerozoley," Izd., A.N. SSSR, 1955.

13. Ludlam, F. H., "The Heat Economy of Rimed Cylinder," Quart. J. R. Met. Soc., Vol. 77, 1951.
14. "Glossary of Meteorology," American Meteor. Soc., Boston, Mass., 1959.
15. Mason, B. J., "The Physics of Clouds," Clar. Press, Oxford, 1971.
16. Hallet, J., "Experimental Studies of the Crystallization of Supercooled Water," J. Atmos. Sc., Vol. 21, 1964.
17. Macklin, W. C. and Ryan, B. F., "The Structure of Ice Grown in Bulk Supercooled Water," J. Atmos. Sc., Vol. 22, 1965.
18. Macklin, W. C., "The Density and Structure of Ice Formed by Accretion," Quart. J. R. Met. Soc., Vol. 88, 1962.
19. Brownscombe, J. L., "Freezing and Shattering of Water Drops in Free Fall," Nature, Vol. 220, 1968.
20. Macklin, W. C. and Payne, G. S., "Some Aspects of the Accretion Process," Quart. J.R. Met. Soc., Vol. 94, 1968.
21. Cohen, M. J. and Richtie, N. J. B. "Low-Speed Three-Dimensional Contraction Design," Journ. Roy. Aero. Soc., Vol. 66, 1962.
22. Schubauer, G. B. and Dryden, H. L., "The Use of Damping Screens for the Reduction of Wind Tunnel Turbulence," Journ. Aero. Sc., April, 1947.
23. Townsend, A. A., "Equilibrium Layers and Wall Turbulence," J. Fl. Mech., Vol. 11, 1961.
24. Pope, A. and Harper, J. J., "Low-Speed Wind Tunnel Design," J. Wiley & Sons, 1966.
25. Bradshaw, P. and Pankhurst, R. C., "The Design of Low-Speed Wind Tunnels," N.P.L. Aero Report No. 1039, 1963.
26. Golitzine, N., "Method for Measuring the Size of Water Droplets in Cloud, Fogs, and Sprays," N.A.E. (Canada) Note 6, 1951.

27. Stallabrass, J. R. and Hearty, P. F., "The Icing of Cylinders of Simulated Freezing Sea Spray," N.R.C. Report MD-50, 1967.
28. Odencrantz, F. K. and Hildebrand, P. H., "A Technique for Direct Measurement of the Size of Small Fog Droplets," J. Appl. Meteor., Vol. 8, 1969.
29. Jones, A. R. and Lewis, W., "A Review of Instruments for the Measurement of the Meteorological Factors Conductive to Aircraft Icing," N.A.C.A. - R.M. No. A9C09, 1949.
30. Neel, C. B., "A Heated Wire Liquid-Water Content Instrument and Results of Initial Flight Tests in Icing Conditions," N.A.C.A. - R.M. No. A54123, 1955.
31. Kármán, T. von, "Turbulence and Skin-Friction," Journ. Aero. Sc., 1934.
32. Wieghardt, K. E. G., "On the Resistance of Screens," Aero. Quart., Vol. 4, 1953.
33. Kays, W. M., "Convection Heat and Mass Transfer," McGraw-Hill, 1966.

APPENDIX A
POWER LOSS CALCULATION

THE PRESSURE LOSS COEFFICIENT

In the straight sections the pressure loss coefficient i.e. the pressure drop Δp in length L is:

$$K = \frac{\Delta p}{L} \kappa \frac{L}{D}$$

where D is hydraulic diameter, κ is the skin friction coefficient. For smooth pipes at high Re (Reynolds Number) Von Kármán [31] gives:

$$1/\kappa = 2 \ln Re \kappa - 0.8$$

It is more suitable to work with a pressure loss coefficient related to the working section speed K_o defined by

$$K_o = K \left(\frac{D_o}{D}\right)^4$$

where D_o is the hydraulic diameter of the working section.

Working Section

Given: $L = 3\text{ft}$, $D = 1.5\text{ft}$, $V = 220\text{ft/sec}$

$Re = 2.05 \times 10^6$, $\kappa = 0.0103$

Hence: $K = 0.0206$, $K_o = 0.0206$

Fan Housing

Given: $L = 6.5$ ft, $D = 3.5$ ft, $V = 40.5$ ft/sec

$Re = 0.87 \times 10^6$, $\kappa = 0.0119$

Hence: $K = 0.0221$, $\underline{K_o = 0.00074}$

Settling Chamber

Given: $L = 3.5$ ft, $D = 6$ ft, $V = 13.8$ ft/sec

$Re = 0.11 \times 10^6$, $\kappa = 0.0130$

Hence: $K = 0.0076$, $\underline{K_o = 0.00003}$

In divergence sections (diffusers) both wall friction and expansion losses occur. The combined losses can be calculated [24] by

$$K = \left(\frac{\kappa}{8 \tan \alpha/2} + 0.6 \tan \alpha/2 \right) \left(1 - \frac{D_1^4}{D_2^4} \right)$$

where α is divergence between opposite walls, D_1 and D_2 are smaller and larger diameter, respectively.

The First Diffuser

Given: $L = 10$ ft, $D_1 = 1.5$ ft, $D_2 = 2.5$ ft, $V_2 = 79$ ft/sec

$Re_2 = 1.22 \times 10^6$, $\kappa = 0.0113$, $\alpha = 5^\circ 40'$

Hence: $K = 0.0498$, $\underline{K_o = 0.0498}$

The Second Diffuser

Given: $L = 8.42$ ft, $D_1 = 2.5$ ft, $D_2 = 3.25$ ft, $V_2 = 47$ ft/sec

$Re_2 = 1.02 \times 10^6$, $\kappa = 0.0117$, $\alpha = 5^\circ 10'$,

Hence: $K = 0.0390$, $K_o = \underline{0.0051}$

The Third Diffuser

Given: $L = 15.67$ ft, $D_1 = 3.25$ ft, $D_2 = 4.92$ ft, $V_2 = 20.5$ ft/sec

$Re_2 = 0.625 \times 10^6$, $\kappa = 0.0125 \times 10^6$, $\alpha = 6^\circ 5'$,

Hence: $K = 0.0497$, $K_o = \underline{0.00226}$

The Wide Angle Diffuser

There is not even an empirical formula for calculation of pressure losses one can rely upon. Assuming the devised diffuser "works" (if it does not, i.e. large separations occur, there must be done "something" with it; e.g. using more dumping screens, anyhow) the pressure loss coefficient will be something in the range 0.3 to 0.5 or less. Let's assume the worst possible case, i.e.

$K = 0.05$, $K_o = \underline{0.00044}$

The Fan Inlet Diffuser

Given: $L = 1.5$ ft, $D_1 = 3.25$ ft, $D_2 = 3.25$ ft, $V_2 = 40.5$ ft/sec

$Re_2 = 0.87 \times 10^6$, $\kappa = 0.0119$, $\alpha = 7^\circ$

Hence: $K = 0.0073$, $K_o = \underline{0.00034}$

The Contraction Cone

In the contraction cone the losses are friction only.

By Pope [24]:

$$K_o = \int_o^{L_c} \kappa \frac{dL}{D} \left(\frac{D_o}{D}\right)^4$$

where L_c is the length of contraction cone. Assuming a mean value for κ ,

$$K_o = 0.32 \kappa L_c / D_o$$

Given: $L_c = 10$ ft, $D_1 = 6$ ft, $D_2 = 1.5$ ft = D_o , $\kappa = 0.013$

Hence: $K_o = 0.02780$

In the corners, both friction and rotation losses occur. For the devised guide vanes Pope [24] suggests this partly empirical relation:

$$K = \left(0.10 + \frac{4.55}{(\ln Re)^{2.58}}\right)$$

The First Corner

Given: $D = 2.5$ ft, $V = 79$ ft/sec, $Re = 1.22 \times 10^6$

Hence: $K = 0.1433$, $K_o = 0.01863$

The Second Corner

Given: $D = 3.25 \text{ ft}$, $V = 47 \text{ ft/sec}$ $Re = 0.95 \times 10^6$

Hence: $K = 0.1455$ $\underline{K_o = 0.00662}$

The Third and Fourth Corners

Given: $D = 6 \text{ ft}$, $V = 13.8 \text{ ft/sec}$. $Re = 0.51 \times 10^6$

Hence: $K = 0.155$, $\underline{K_o = 0.00605}$

The Cooler

As quoted by the manufacturer of the coils
(Climatrol, Toronto) the required cooler has

$$\underline{K_o = 0.078}$$

For the screens Weighardt [32] suggests the following
formula for calculation of the resistance coefficient:

$$K = 6(1 - B)B^{-5/6} Re^{-1/3}$$

where

$$B = \frac{\text{area of holes}}{\text{total area}} = \left(1 - \frac{d}{l}\right)^2$$

where l denotes the width of the square mesh, and d is wire
diameter; Re is the Reynolds number based on the wire
diameter.

The Settling Chamber Screens

Given: $d = 0.016$ inch, $l = 0.05$ inch, $B = 0.462$, $Re = 114$

Hence: $K = 1.27$, $\underline{K_o = 0.00495}$

At most 10 screens can be used, hence

$$\underline{K_o = 0.0495}$$

The First Safety Screen

Given: $D = 2.5$ ft, $d = 0.04$ inch, $l = 0.5$ inch, $B = 0.845$

$Re = 1635$

Hence: $K = 0.0906$, $\underline{K_o = 0.01180}$

The Second Safety Screen

Given: $D = 3.25$ ft, $d = 0.04$ inch, $l = 0.5$ inch, $B = 0.845$,

$Re = 835$

Hence: $K = 0.1135$, $\underline{K_o = 0.00505}$

THE TOTAL PRESSURE LOSS COEFFICIENT

$$\underline{\Sigma K_o = 0.2722}$$

THE ENERGY RATIO

$$\underline{ER = 1/\Sigma K_o = 3.67}$$

THE TOTAL ENERGY LOSS

$$\Delta E = \frac{1}{2} \rho A_o V_o^3 \Sigma K_o$$

where A_o and V_o are cross-sectional area and speed of the testing section, respectively; ρ being the density of air.

We have

Given: $\rho = 0.00234 \text{ slug/ft}^3$, $A_o = 1.86 \text{ ft}^2$, $V_o = 220 \text{ ft /s}$

Hence:

$$\begin{aligned} \underline{\Delta E} &= 6307.47 \text{ lb ft /s} \\ &= \underline{11.47 \text{ hp}} \end{aligned}$$

THE TOTAL STATIC PRESSURE LOSS

$$\begin{aligned} \underline{\Delta p} &= \frac{1}{2} \rho V_o^2 \Sigma K_o \\ &= 15.4 \text{ lb/ft}^2 \\ &= \underline{2.96 \text{ inch. H}_2\text{O}} \end{aligned}$$

SELECTION OF THE FAN

The maximum volume flow through testing section is

~ 25,000 cfm at 150 mph

The total static pressure drop is

~ 3 inch of H_2O

A fan which meets the above requirements as well as the others - namely, safe operation under wet and icy conditions, and the price-is:

Vaneaxial Direct Driven Fan - catalogue number

V 421 - X 42 - designed by

Aerovent Fan Company, Inc., Pigua, Ohio, U.S.A.,

manufactured under licence by

Powlesland Engineering Ltd., Woodbridge, Ontario.

The above fan, originally equipped with 20 hp motor, is a constant volume machine, i.e. regardless of air density changes it gives constant volume flow. As a result if the fan operates at lower temperatures the horsepower changes in direct proportion to the density. The lowest temperature the fan will be run at is - 40°C; hence the appropriate density ratio (density of air at -40°C to density at + 20°C) is 1.3. The required horsepower then is

$$1.3 \times 20 = \underline{26 \text{ hp}}$$

However, since there were available only 25 and 30 hp motors, the latter has been chosen.

APPENDIX B
HEAT LOSS CALCULATION

Heat Loss to the Environment (Q_e)

$$Q_e = HA (T_o - T_i)$$

where

$A = 1050 \text{ ft}^2$ is overall outside surface area of the tunnel body.

$T_i = -40^\circ\text{F}$ is lowest operation temperature

$T_o = + 72^\circ\text{F}$ is room temperature, and H is overall heat transfer coefficient defined by

$$H = \frac{1}{\frac{1}{h_i} + \frac{t}{k} + \frac{1}{h_o}}$$

where h_i , h_o are (convection) heat transfer coefficients related to convection inside or outside of the tunnel, respectively, t , k are the thickness and thermal conductivity of the insulation, respectively.

h_i in the above formula has been neglected since its relatively high value (forced convection) becomes unimportant with respect to the remaining terms.

h_o has been evaluated considering free convection from horizontal cylinders and an equivalent diameter of the tunnel, the latter defined by

$$D_e = \frac{1}{V_o} \sum_i D_i V_i$$

the actual value of D_e has been found

$$D_e = 2.95 \text{ ft.}$$

the Grashof No.

$$\text{Gr} = 2.34 \times 10^9,$$

the Prandtl No.

$$\text{Pr} = 0.712$$

the Nusselt number [33]

$$\begin{aligned} \text{Nu} &= 0.13 (\text{Gr Pr})^{1/3} \\ &= \underline{140} \end{aligned}$$

hence

$$\underline{h_o = 0.74 \text{ Btu/hr ft}^2\text{°F}}$$

As the insulation material polyurethane was used with:

$$k = 0.13 \text{ Btu/hr ft}^2\text{°F}$$

hence (for $t = 1$ inch):

$$H = 0.38 \text{ Btu/hr ft}^2\text{°F}$$

and

$$\underline{Q_{1e} = 43,900 \text{ Btu/hr}}$$

For $t = 2$ inch:

$$H = 0.304 \text{ Btu/hr ft}^2\text{°F}$$

and

$$\underline{Q_{2e} = 35,300 \text{ Btu/hr}}$$

For $t = 3$ inch:

$$H = 0.256 \text{ Btu/hr ft}^2\text{°F}$$

and

$$\underline{Q_{3e} = 29,500 \text{ Btu/hr}}$$

Dissipation of Energy (Q_d)

This represents rather simple calculations; the fan is driven by a 30 hp motor so at most all this energy could dissipate through viscous friction. Thus the maximum loss could be

$$\underline{Q_d = 76,500 \text{ Btu/hr}}$$

Extraction of the Latent Heat from the Spray (Q_1)

The maximum flow rate of water through spray nozzles of

$$60 \text{ gm/s}$$

is being considered which results in requirement of

$$\underline{Q_1 = 57,200 \text{ Btu/hr}}$$

for the refrigeration unit capacity.

Sensible Cooling of the Spray

Sensible cooling of the water before the nozzles

$$Q_{sw} = 14,200 \text{ Btu/hr}$$

"provided the water enters the tunnel" at +20°C.

Sensible Cooling of the Ice Deposit

$$Q_{si} = 7,100 \text{ Btu/hr}$$

provided the ice deposit temperature is -20°C.

Hence the total heat for sensible cooling of the spray is

$$Q_s = 21,400 \text{ Btu/hr}$$

Finally the total heat capacity requirement for the refrigeration unit is

$$\begin{aligned} Q &= 199,000 \text{ Btu/hr} \\ &= \underline{16,6 \text{ tons of refrigeration}} \end{aligned}$$

Selection of the Refrigeration unit

As mentioned before since the first stage of experimental program will be carried out at higher temperatures, at most - 20°C, lower velocities, up to 90 mph, and also at lower water flow rates of the spray, up to 30 g/s, an alternative calculation of heat losses has been performed giving

Heat loss to environment

$$Q_e = 36,000 \text{ Btu/hr}$$

Dissipation of energy through friction

$$Q_d = 23,000 \text{ Btu/hr}$$

Extraction of latent heat from the spray

$$Q_l = 34,200 \text{ Btu/hr}$$

Sensible cooling of the spray

$$Q_s = 12,900 \text{ Btu/hr}$$

Hence the total heat loss

$$\begin{aligned} Q &= 106,100 \text{ Btu/hr} \\ &= \underline{8185 \text{ tons of refrigeration}} \end{aligned}$$

Based on the above the following unit has been chosen:

(1) 5H40 Carrier Refrigeration Compressor of rating:

Capacity: 8.7 tons

SST/502: -20°F

SCT/502: $+110^{\circ}\text{F}$

Brake hp: 19.9

where SST/502 x SCT/502 are saturated suction, or condensing temperature using refrigerant 502, respectively

(2) 5F30 Carrier Water Cooled Condensor of rating:

Total heat rejection: 13.2 tons

Water flow rate: 16 gpm at -70°F

Pressure drop: 6.9 ft.

both designed and manufactured by

Carrier Air Conditioning Co.

Syracuse, New York, U.S.A.

(3) Climatrol Evaporator 72 x 72 inch. matched with the compressor; designed and manufactured by

Climatrol Air Coils Ltd.

Oakville, Ontario, Canada.

For the extension to -40°C (design data and ratings) use Carrier Application Data Bulletin, Form 5F, H - 2XA/1968.